MODEL
INTER-COMPARISON
on
TRANSPORT
and
CHEMISTRY

report on model inter-comparison performed within European Commission FP5 project EVERGREEN
("Global satellite observation of greenhouse gas emissions")

Evergreen

MODEL
INTER-COMPARISON
on
TRANSPORT
and
CHEMISTRY

EVERGREEN partners (modeling):
P. Bergamaschi[1]
J.F. Meirink[2]
J.F. Müller[3]
S. Körner and M. Heimann[4]

external partners (modelling):
P. Bousquet[5]

external partners (surface measurements):

E.J. Dlugokencky[6], U. Kaminski[7], R. Vecchi[8]
G. Marcazzan[8], F. Meinhardt[9], M. Ramonet[5],
H. Sartorius[10], W. Zahorowski[11]

joint research centre
EUROPEAN COMMISSION

[1] European Commission, DG Joint Research Centre, Institute for Environment and Sustainability, Ispra, Italy
[2] Royal Netherlands Meteorological Institute, de Bilt, the Netherlands
[3] Belgian Institute for Space Aeronomy, Brussels, Belgium
[4] Max Planck Institute for Biogeochemie, Jena, Germany
[5] Laboratoire des Sciences du Climat et de l'Environment (LSCE), Gif sur Yvette, France
[6] NOAA Earth Science Research Laboratory, Global Monitoring Division, Boulder, CO, USA
[7] Deutscher Wetterdienst, Meteorologisches Observatorium Hohenpeissenberg, Germany
[8] Istituto di Fisica Generale Applicata - Universita' degli Studi di
Milano, Italy
[9] Umweltbundesamt, Messstelle Schauinsland, Kirchzarten, Germany
[10] Bundesamt für Strahlenschutz, Freiburg, Germany
[11] Australian Nuclear Science and Technology Organisation, Menai, Australia

Contact

Peter Bergamaschi
European Commission
DG Joint Research Centre
Institute for Environment and Sustainability (IES)
Climate Change Unit
TP 280
I-21020 Ispra (Va)
Tel.   +39 0332 789621
peter.bergamaschi@jrc.it

Document also available on the JRC/IES/CCU world wide web site at:
http://ccu.jrc.it/

The mission of the Institute for Environment and Sustainability is to provide scientific and technical support to the European Union's policies for protecting the environment and the EU Strategy for Sustainable Development.

CONTENTS

1 Executive summary

A comprehensive inter-comparison of 5 atmospheric chemistry transport models (TM5, TM4, TM3, IMAGES, and LMDZ) has been performed. The main objective was to analyze differences in model transport, in particular vertical mixing (boundary layer and convective transport), synoptic variations, and large scale global circulation (including inter-hemispheric exchange and stratospheric tropospheric exchange (STE)). For this purpose simulations of various tracers with very different atmospheric lifetimes τ have been carried out: ^{222}Rn ($\tau = 3.8$ days), SF_6 ($\tau = \sim 3000$ years), and CH_4 ($\tau = \sim 9$ years), using prescribed boundary conditions for all models. Furthermore, OH fields from various model simulations with full chemistry have been compared.

^{222}Rn simulations show significant differences in vertical transport between models, leading to differences of simulated ^{222}Rn concentrations near the surface of up to a factor of ~ 3. The TM5 and TM4 model have generally the highest ^{222}Rn concentrations near the surface, while the other models tend to stronger vertical mixing. Comparison with in-situ measurements at 9 surface monitoring sites show that synoptic variations are simulated relatively well by all models which use (re)analyzed meteorological fields (i.e. all models except IMAGES, which is using monthly mean climatological fields). Comparison of TM5 and TM4 simulations (which have the same parameterization of atmospheric transport) illustrate that increasing horizontal model resolution significantly improves agreement with observations.

Simulations of SF_6 show significant differences in inter-hemispheric transport between the applied models, ranging between 6 and 12 months. This range is consistent with previous model inter-comparisons, e. g. within TransCom2 [*Denning et al.*, 1999]. STE is weaker and probably more realistic (15–16 months) in TM5, TM4, and LMDZ than in TM3 and IMAGES (7-8 months). The difference in STE between TM3 vs. TM5/TM4 is probably largely due to the different vertical resolution of the applied model versions.

CH_4 tracer simulations with prescribed OH fields were performed for TM5, TM4 and IMAGES. Consistent with the ^{222}Rn simulations, TM5 and TM4 show higher CH_4 mixing ratios near the surface over CH_4 source regions compared to IMAGES. Both TM5 and TM4 simulate synoptic variations very well at most surface monitoring sites. Similar as for the ^{222}Rn experiments agreement with CH_4 surface observations is improving with increasing horizontal model resolution. The large difference in STE between TM5/4 and IMAGES is also clearly reflected in the CH_4 simulations.

Furthermore, OH distributions have been compared from model simulations with full chemistry. For these simulations the applied models (TM5, TM4, IMAGES) used different emission inventories (representing typical standard configurations of the corresponding models). Simulated OH fields show significant differences near the surface, probably largely due to the applied different emission inventories (CO, NMHC, NO_x). In the free troposphere, however, the spatial OH distribution are relatively similar. In addition, also the seasonal OH variation is very consistent for all model runs. Global CH_4 + OH lifetimes in the range of 8.3 - 11.4 years have been calculated for the different OH fields. All models suggest 20-40% higher CH_4 lifetime in the SH, compared to NH.

2　Atmospheric models

The applied atmospheric transport and chemistry models are listed in Table 2.1.

Table 2.1: Applied atmospheric models

model	TM5 (JRC)	TM4[1] (KNMI)	TM3 (MPI)	IMAGES (BIRA-IASB)	LMDZ (CNRS-LSCE) external partner
horizontal resolution	6 x 4 (global) 1 x 1 (zoom over Europe)	3 x 2	5 x 3.8	5 x 5	3.75 x 2.5
vertical layers	25 hybrid	25 hybrid	19 sigma	25 sigma	38
advection	slopes scheme [*Russell and Lerner*, 1981]	slopes scheme [*Russell and Lerner*, 1981]	slopes scheme [*Russell and Lerner*, 1981]	Semi-Lagrangian (2nd order) [Smolarkiewicz and Rasch, 1991]	finite-volume second-order scheme [Van Leer , 1977; Hourdin and Armengaud, 1999]
vertical diffusion	PBL:[*Holtslag and Moeng*, 1991] FT: [*Louis*, 1979]	PBL: [*Holtslag and Moeng*, 1991] FT:[*Louis*, 1979]	[*Louis*, 1979]	PBL: [Muller and Brasseur, 1995]	PBL: Mass Flux Representation of Thermals [Hourdin et al., 2002]
convective cumulus clouds	[*Tiedtke*, 1987]	[*Tiedtke*, 1987]	[*Tiedtke*, 1987]	[Muller and Brasseur, 1995] [Costen et al., 1988]	[*Tiedtke*, 1987]
meteorology	ECMWF	ECMWF	NCEP	ECMF (climatological)	GCM, nudged to ECMWF
chemistry	- offline - CBM4 based chem	- offline - CBM4 based chem	- offline	- offline - IMAGES-chemistry	- offline - [Hauglustaine et al., 2004]
model reference	[*Krol et al.*, 2005]	[Dentener et al., 2003]	[*Heimann and Koerner*, 2003]	[Muller and Brasseur, 1995]	
222Rn	●	●	●	●	●
SF6	●	●	●	●	●
OH	●	●		●	
CH4	●	●		●	

[1] in some plots of this report the previous name 'TM3_KNMI' is still used; however the applied model version is identical as described for 'TM4_KNMI'.

3 ^{222}Rn intercomparison

3.1 ^{222}Rn modelling protocol

^{222}Rn emissions
Similar to other ^{222}Rn studies constant ^{222}Rn emissions are assumed over land surfaces (between -60° S and 60° N ^{222}Rn emissions of 1 atom cm^{-2} s^{-1}; between 60° N and 70° N emissions of 0.5 atom cm^{-2} s^{-1}). For all other land surfaces (incl. Greenland and Antarctica) and for the ocean emissions are set to zero.

^{222}Rn sink
radioactive decay: rate constant k = 2.11E-6 [s^{-1}]

Initialization and simulation period
simulation period: 2001 (1 full year, spin-up 1 month)
initialization: ^{222}Rn (01.12.2000) = 0.0

3.2 ^{222}Rn results

The 3D distributions of simulated ^{222}Rn concentrations are illustrated in Fig. 3.1 (surface), Fig 3.2 (free troposphere at 500 hPa), and Fig 3.3 (vertical distribution). In particular near the surface significant differences are visible between the models. The TM5 and TM4 model have generally the highest ^{222}Rn concentrations near the surface, while the other models tend to stronger vertical mixing. In December, the LMDZ model has similar surface ^{222}Rn concentrations as TM5 and TM4 over the extratropical NH landmasses, but much lower values over the tropics. The displayed surface values represent the concentrations of the lowest model layer. Therefore, beside differences in vertical mixing, also differences in vertical model resolution may play a role, e.g. when comparing TM5/TM4 with TM3. While many parameterizations are identical or similar between TM5/TM4 and TM3 (such as vertical diffusion in the free troposphere, and convective cumulus clouds), TM5/TM4 apply the diffusion parameterization of [Holtslag and Moeng, 1991] in the PBL, use ECMWF meteorological fields (compared to NCEP in TM3) and have higher vertical resolution. As expected 3D distributions of TM5 and TM4 are very similar (as for the other tracer experiments with SF$_6$ and CH$_4$), but effects due to the different horizontal resolution (TM5 6°x4^o; TM4: 3°x2^o) are clearly visible near the surface.
Model simulations have been compared with ^{222}Rn measurements at 9 European and global monitoring sites (Fig. 3.4). Synoptic variations are simulated relatively well by all models which use (re)analyzed meteorological fields (i.e. all models except IMAGES, which is using monthly mean climatological fields). At the two European continental sites Freiburg and Milano, also the simulated average diurnal variations (mainly due to the diurnally varying boundary layer) agree very well with observations, in particular for TM5 and TM4. TM3 and LMDZ also show these diurnal cycles, but simulate lower mean concentrations than observations. In general very difficult to simulate are sites at the land-sea border (as Mace Head) and mountain sites. For some of these sites, sampling locations were slightly shifted in some models. E.g. at Mace Head, the sampling point has been shifted 2-3° westwards in some models (avoiding or reducing the effect of local ^{222}Rn emissions of the

corresponding model grid cell), leading to significant improvements with observations.

Several mountain sites (in particular Zugspitze) exhibit significant influence of local mountain-valley winds, which with the applied models cannot be reproduced. Comparison of TM5 and TM4 simulations (which have the same parameterization of atmospheric transport) show that increasing horizontal model resolution significantly improves agreement with observations (Fig. 3.5). On the global domain TM4 achieves higher correlation with measurements than TM5 (resolution 3^ox2^o (TM4) vs. 6^ox4^o (TM5)), on the European zoom domain the correlation for TM5 is higher (1^ox1^o (TM5) vs. 3^ox2^o (TM4)).
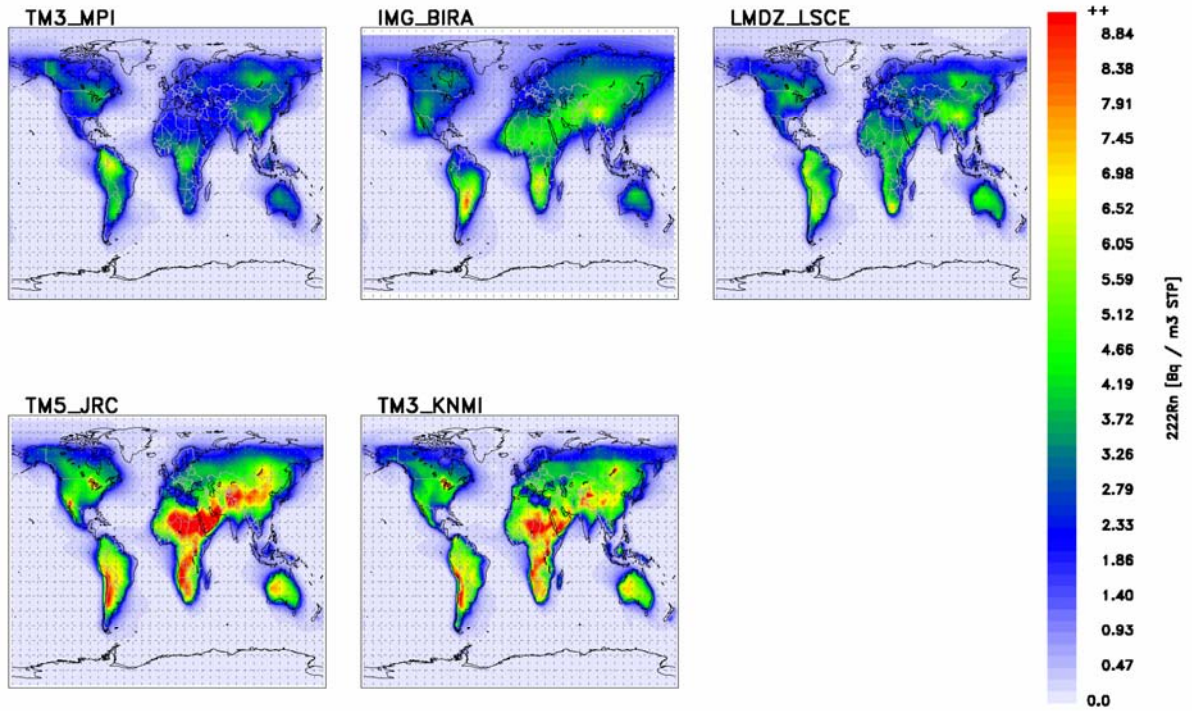
surface   June

surface   December
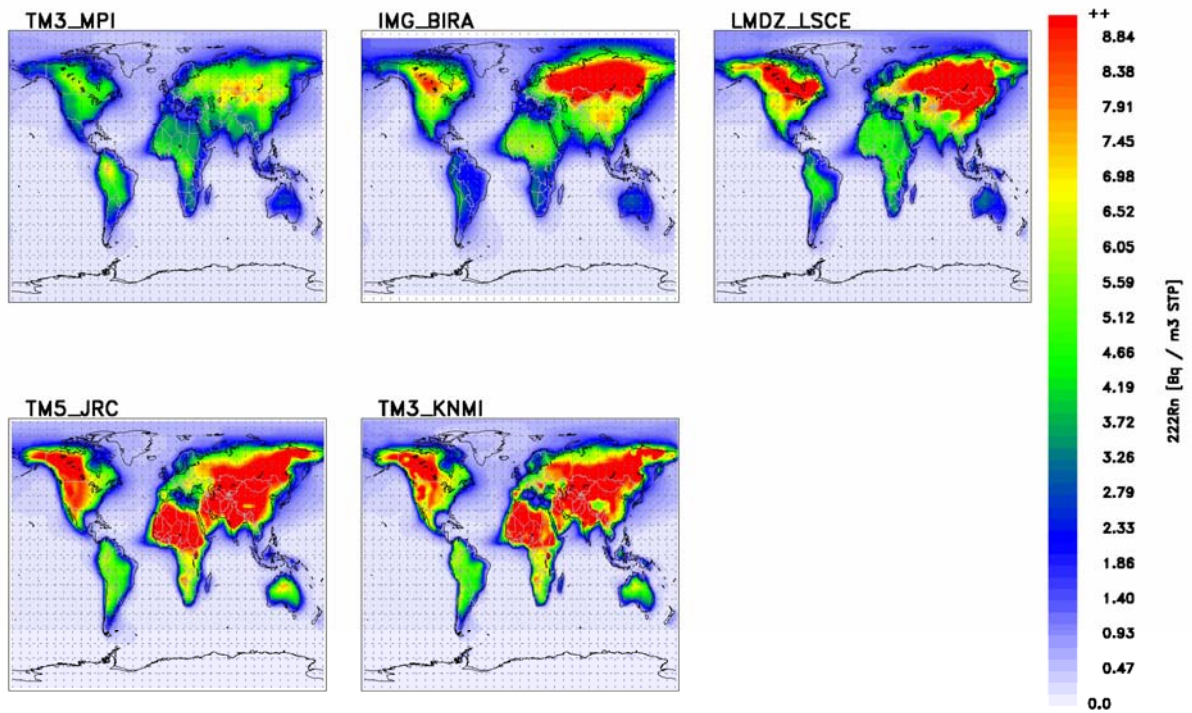
Figure 3.1: [222]Rn intercomparison: surface (top: June 2001; bottom: December 2001).
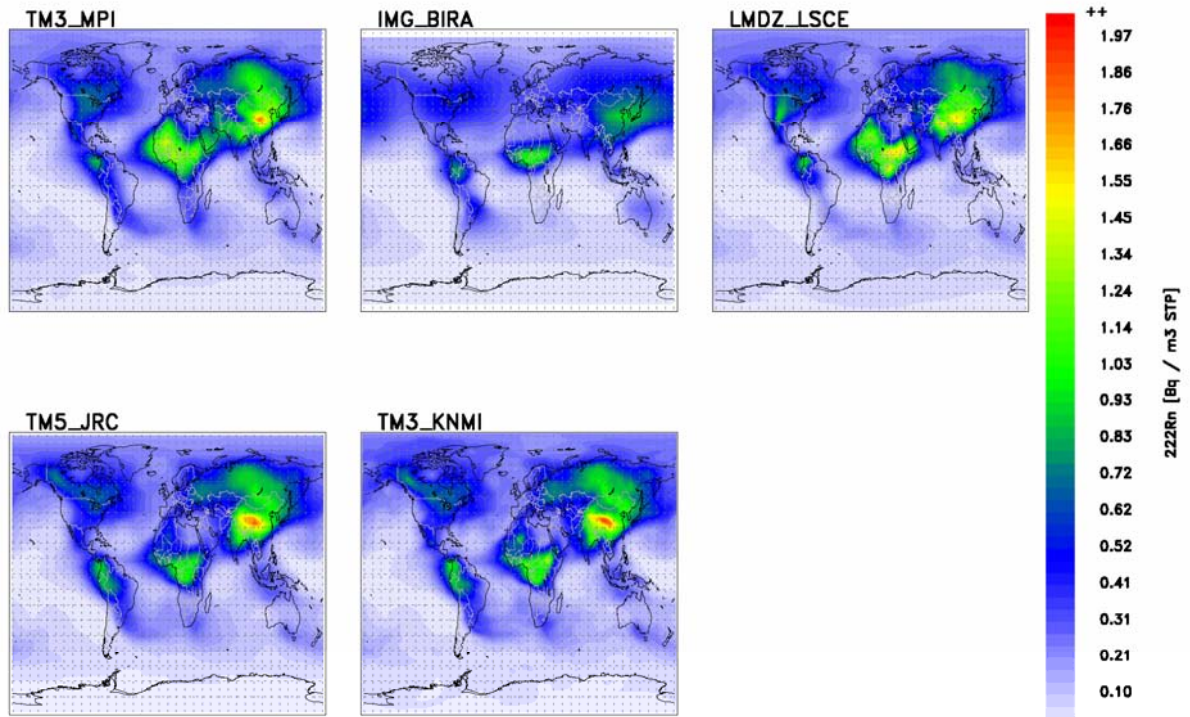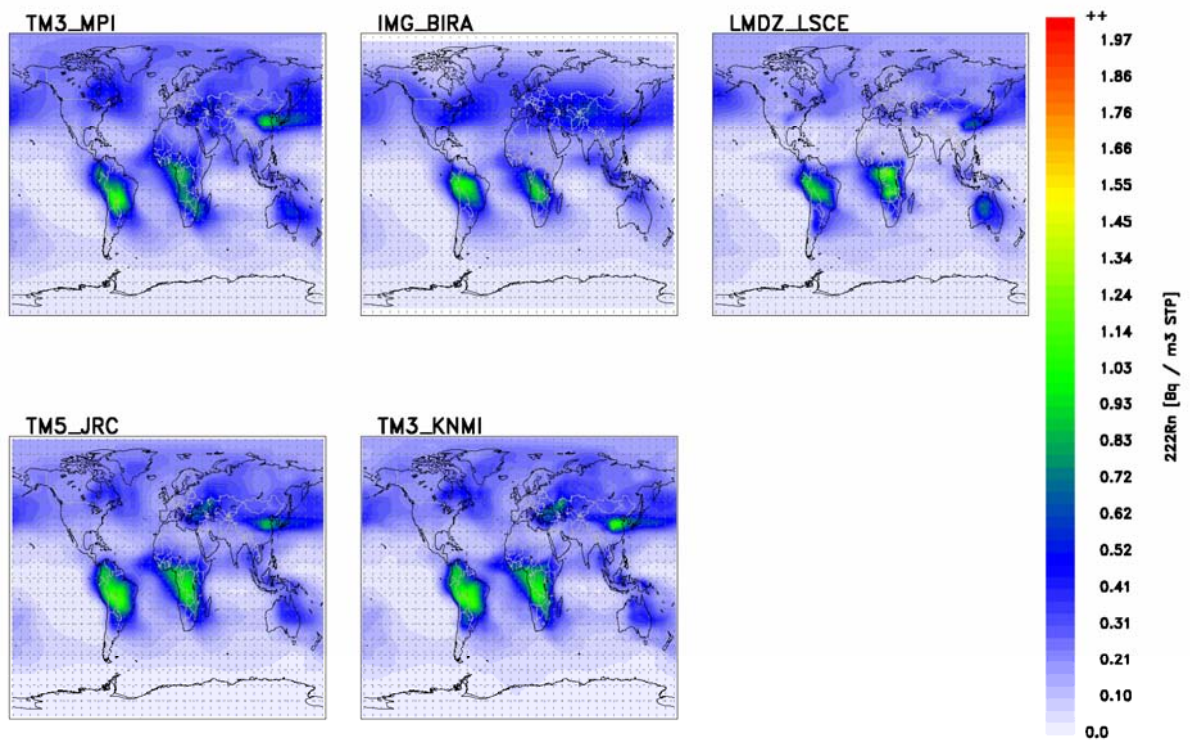
Figure 3.2: [222]Rn intercomparison: free troposphere (500 hPa) (top: June 2001; bottom: December 2001).
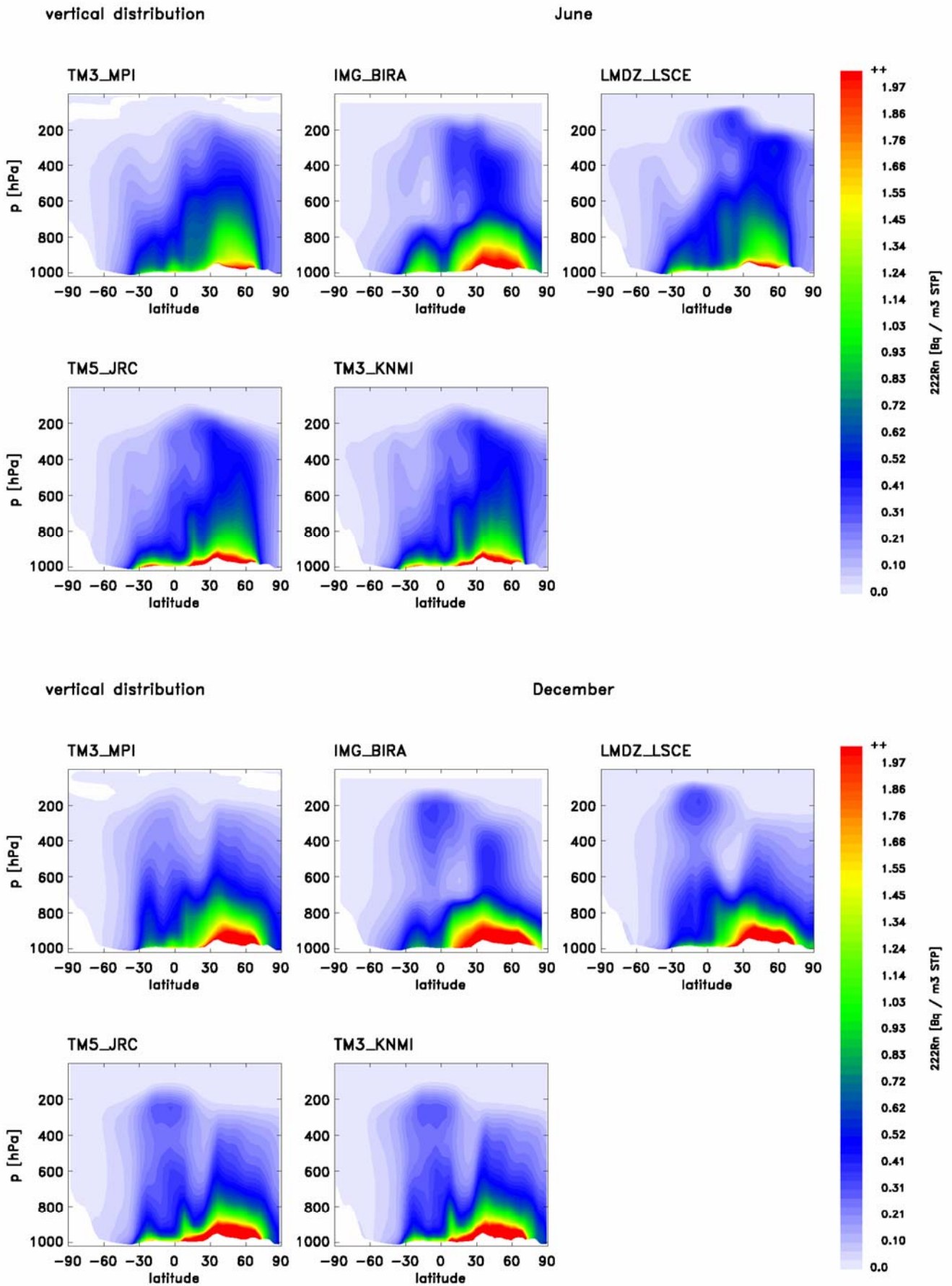
Figure 3.3: [222]Rn intercomparison: vertical distribution (latitudinal averages) (top: June 2001; bottom: December 2001).
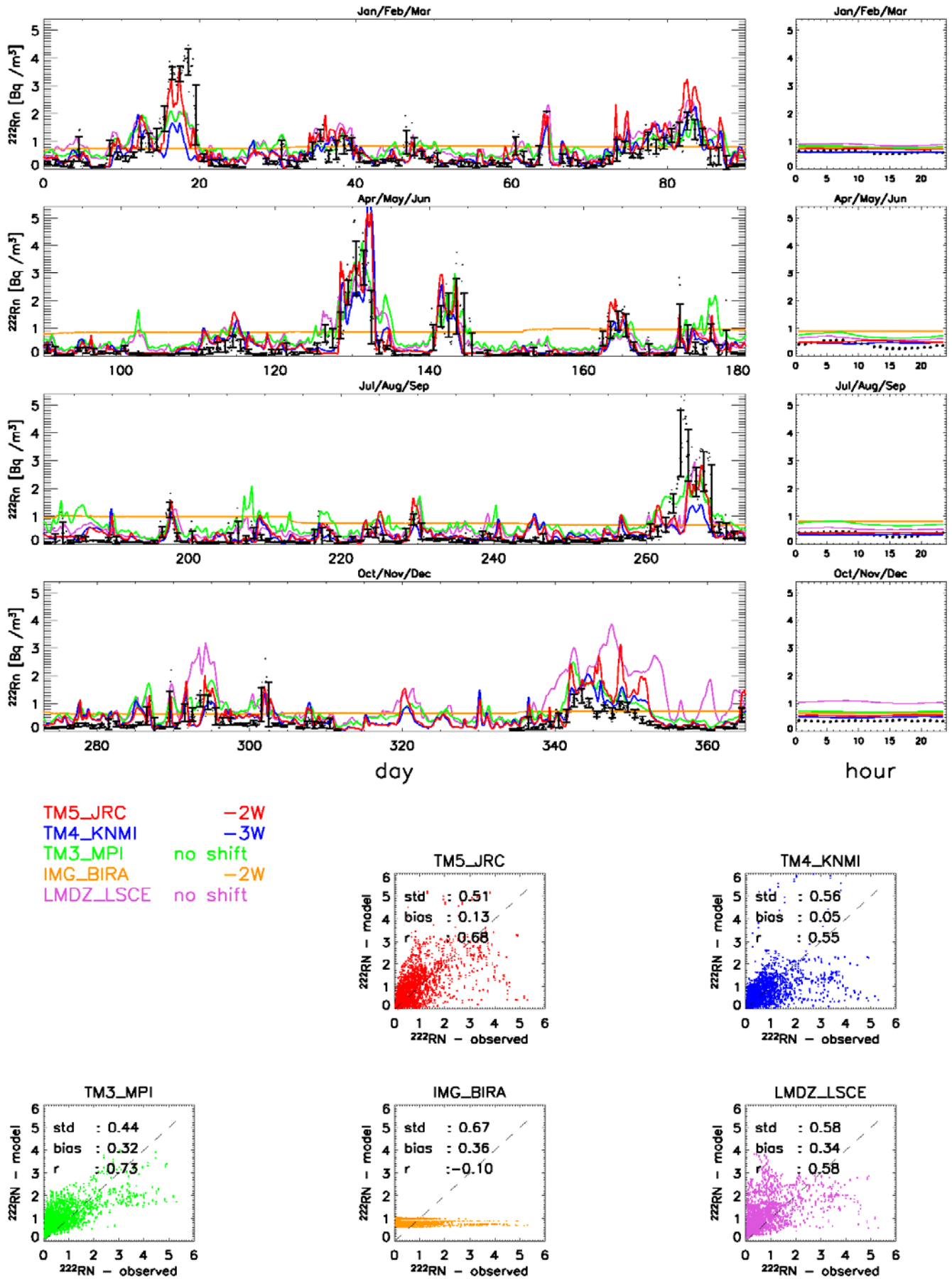
Figure 3.4: ^{222}Rn intercomparison: Surface monitoring stations.
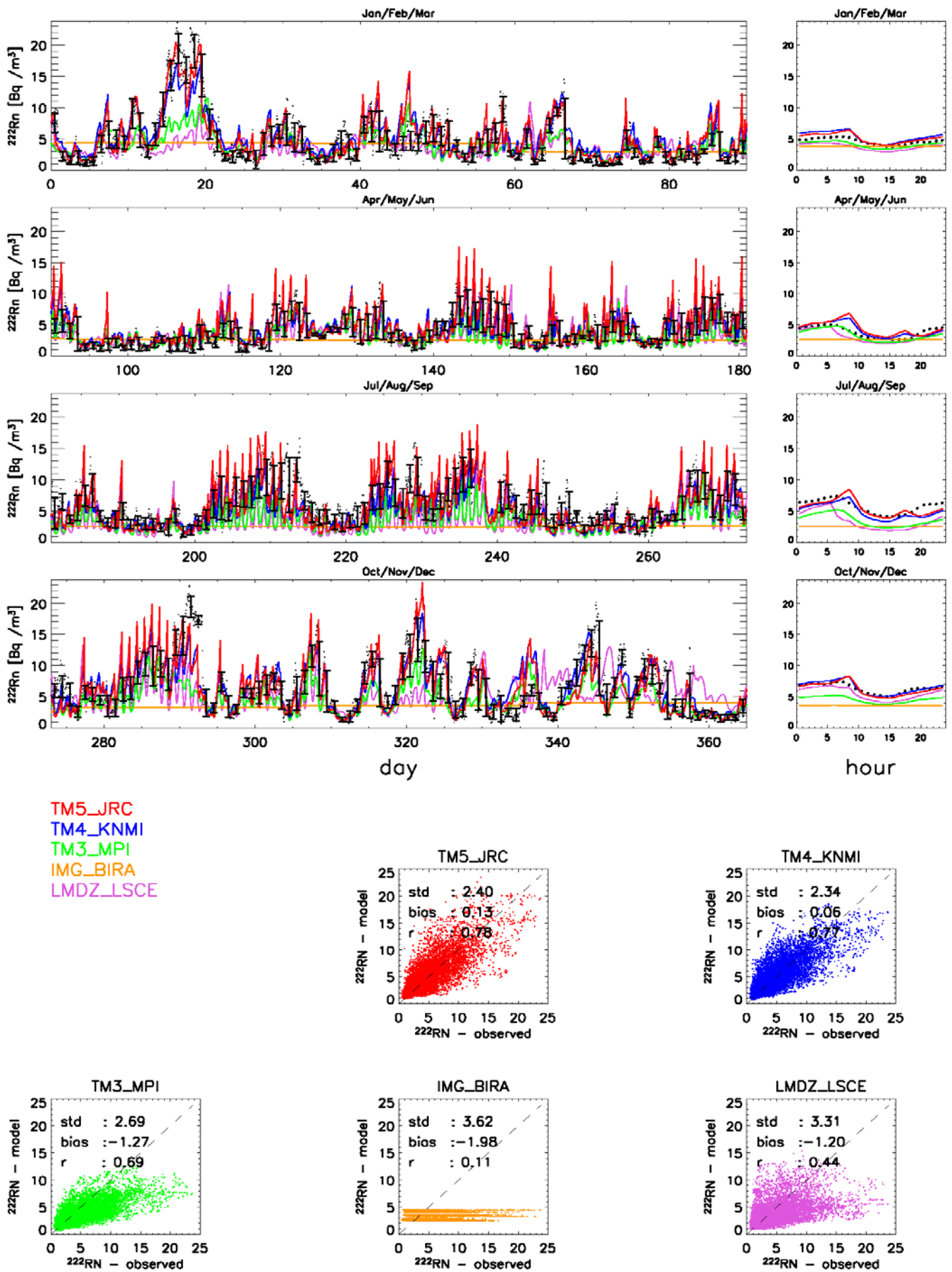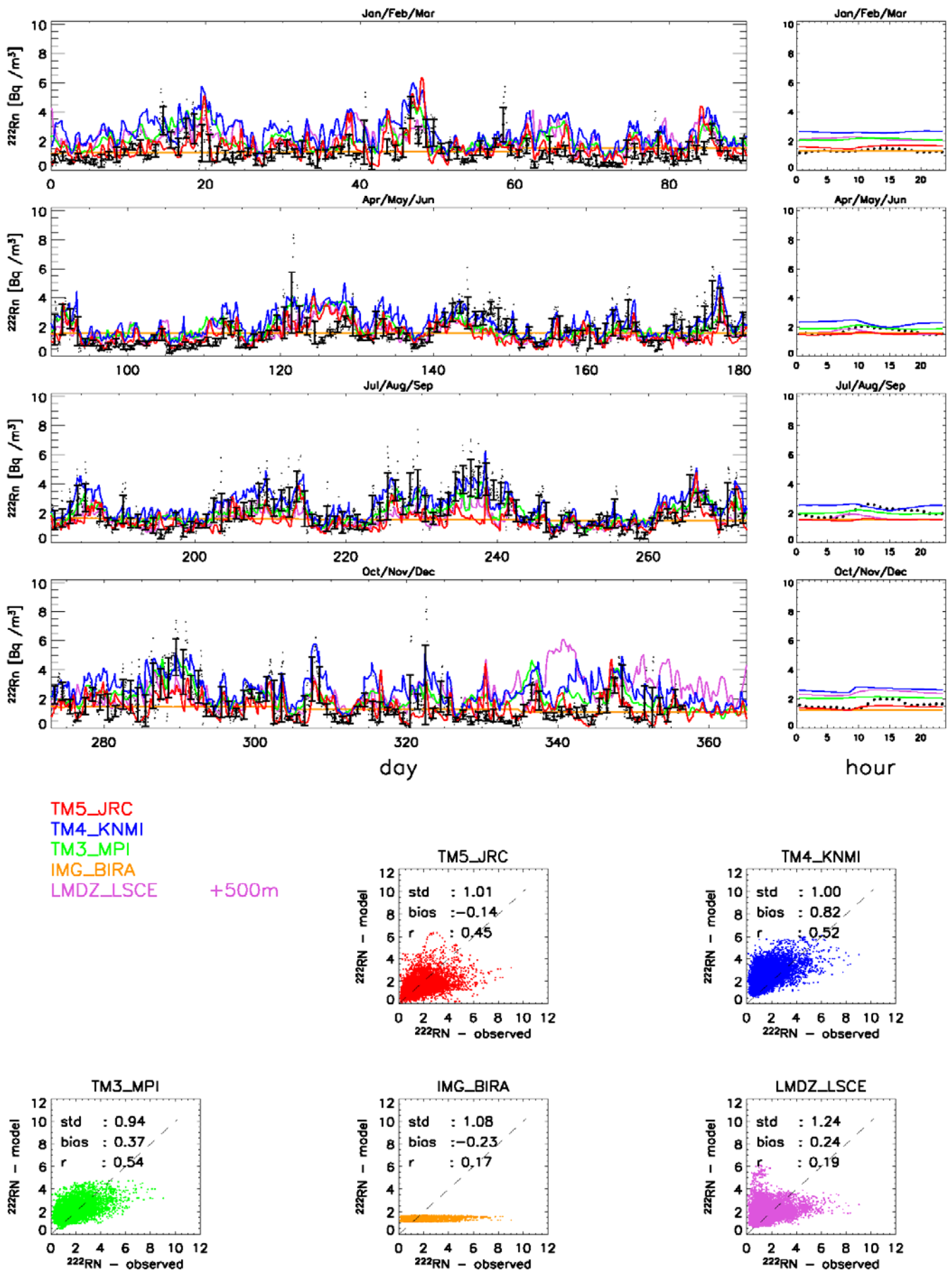
FRB_BFS(48.00 N, 7.85 E, 276.0 m asl) Freiburg, Germany   2001

Figure 3.4: continued.

Figure 3.4: continued.

Figure 3.4: continued.

Figure 3.4: continued.

Figure 3.4: continued.

Figure 3.4: continued.

AMS_CEA(−37.95 N, 77.53 E, 150.0 m asl) Amsterdam Island, France   2001
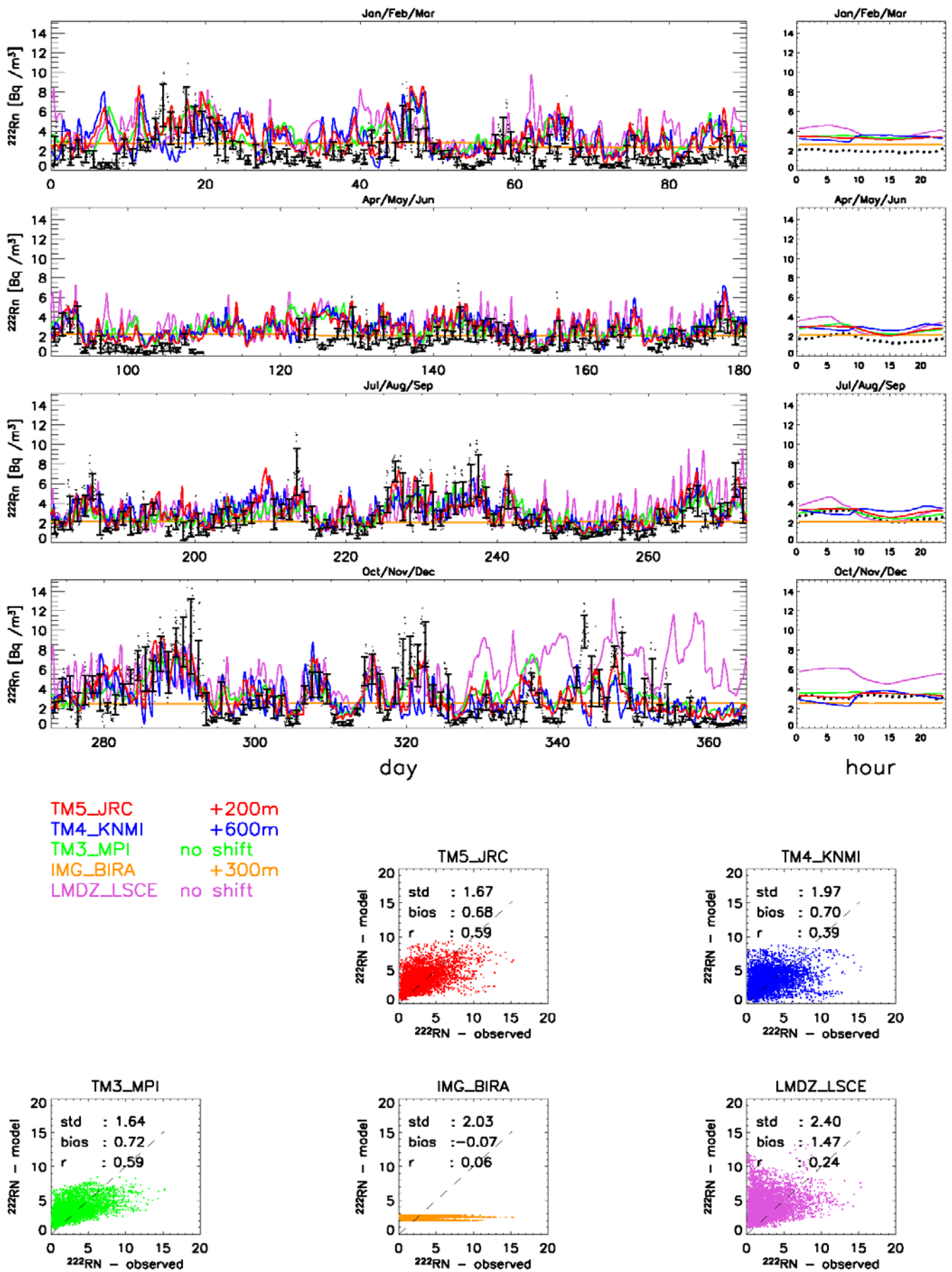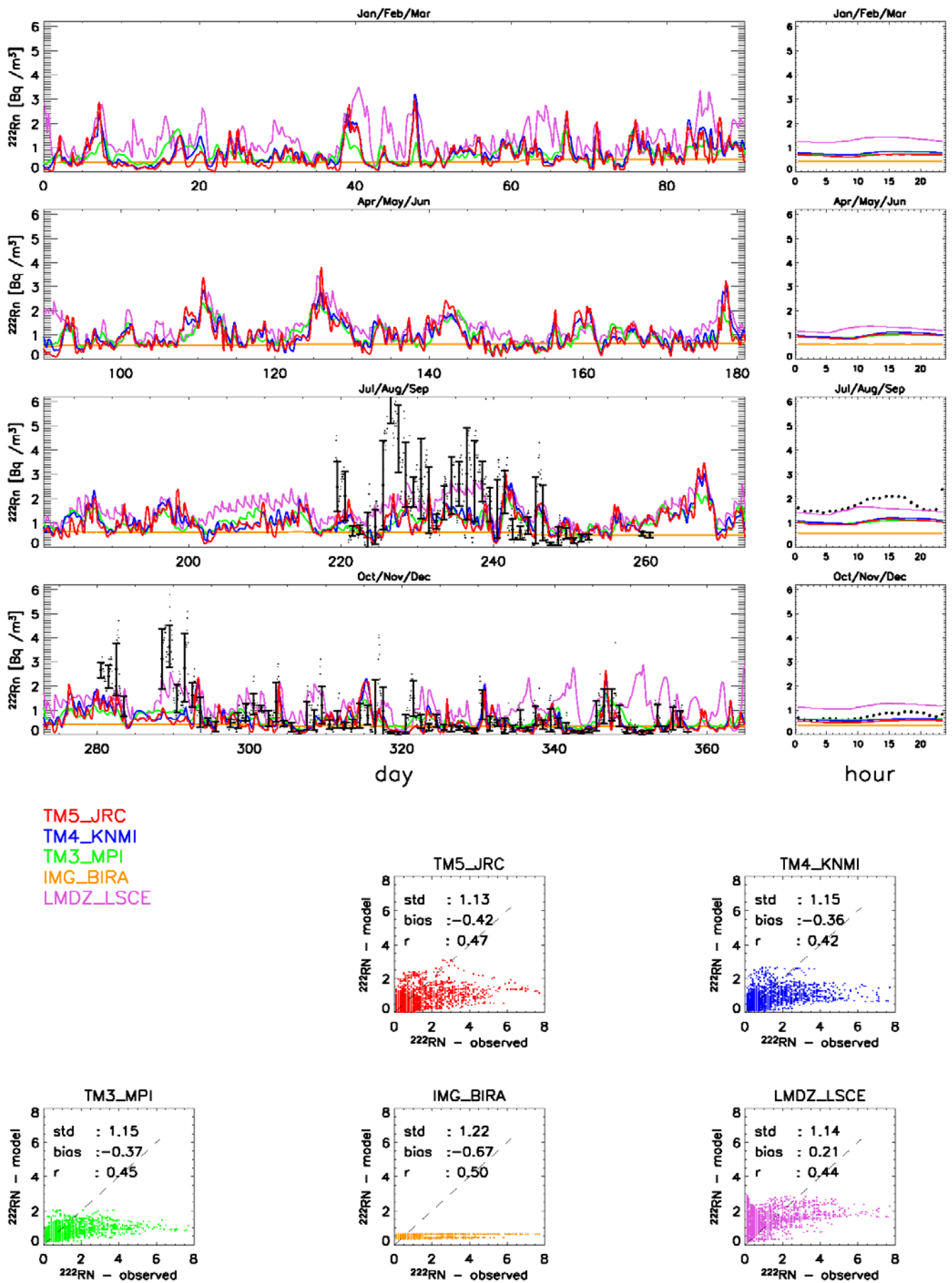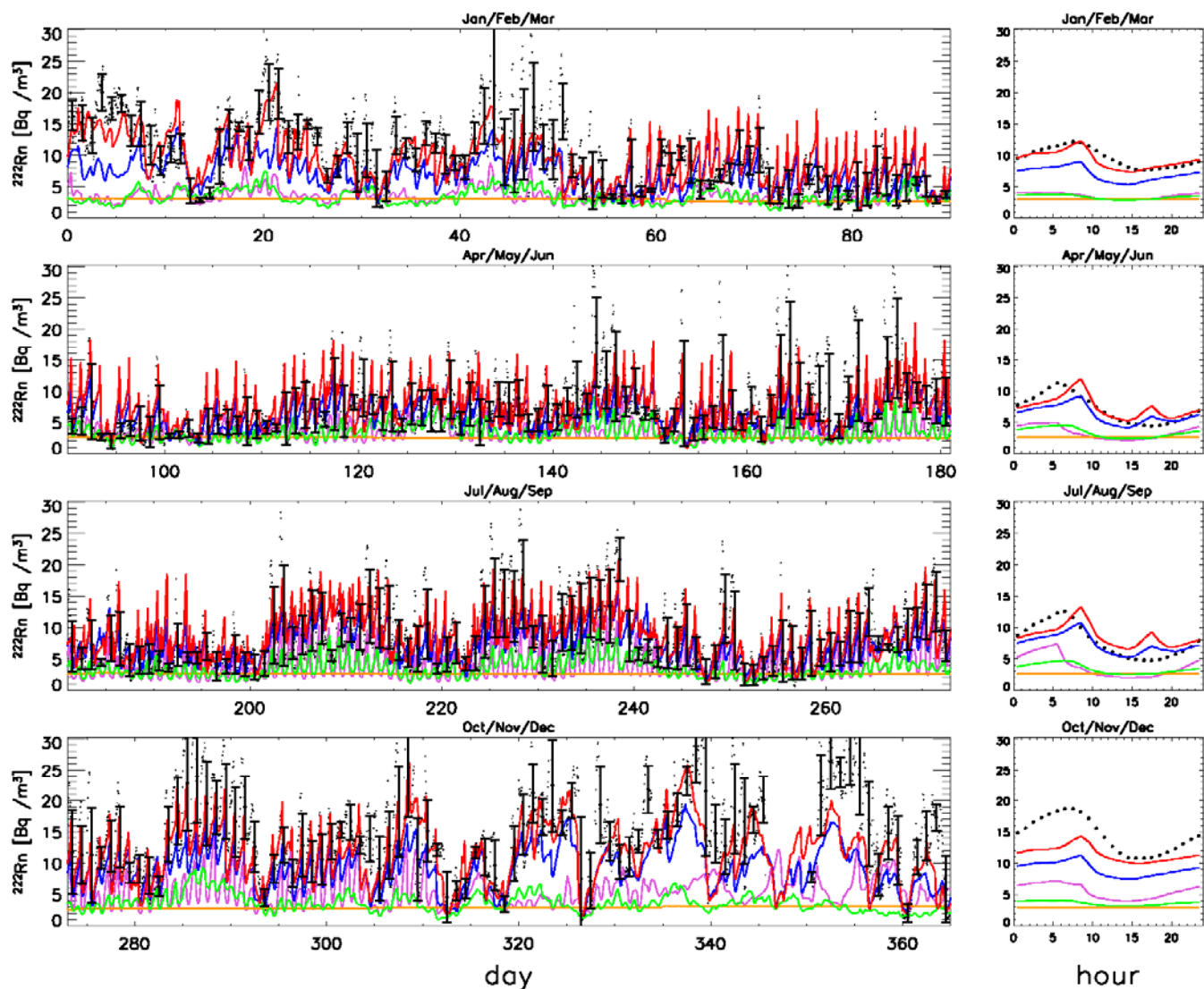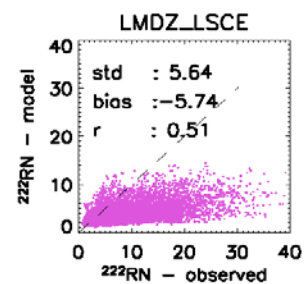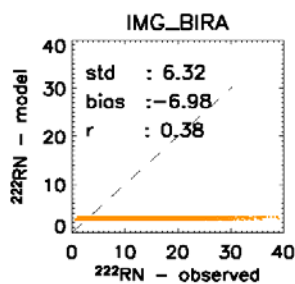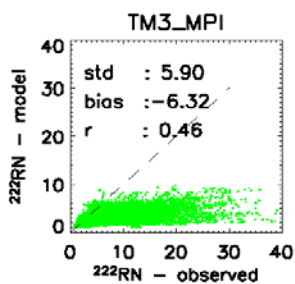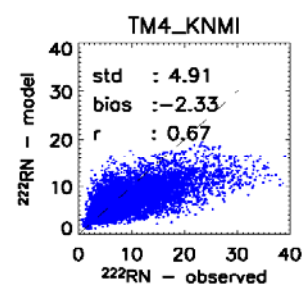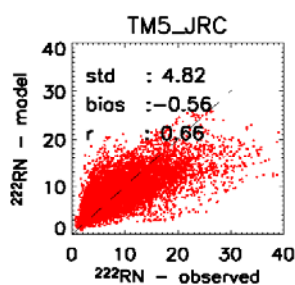
TM5_JRC
TM4_KNMI
TM3_MPI
IMG_BIRA
LMDZ_LSCE

Figure 3.4: continued.

CGO_ANS(−40.68 N, 144.69 E, 164.0 m asl) Cape Grim, Australia (70m AGL)   2001

TM5_JRC
TM4_KNMI
TM3_MPI
IMG_BIRA
LMDZ_LSCE

TM5_JRC
std : 0.79
bias : 0.16
r   : 0.69

TM4_KNMI
std : 0.72
bias : 0.36
r   : 0.76

TM3_MPI
std : 0.79
bias : 0.09
r   : 0.69

IMG_BIRA
std : 1.09
bias : 0.39
r   : −0.18

LMDZ_LSCE
std : 0.76
bias : 0.16
r   : 0.73
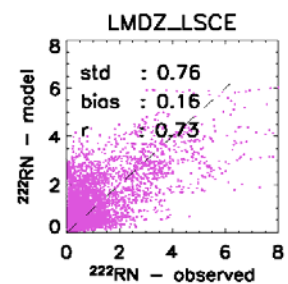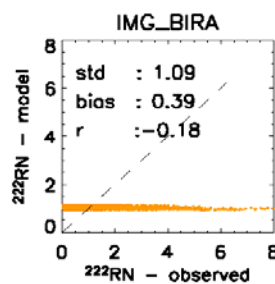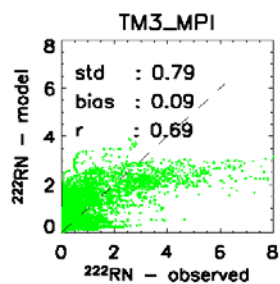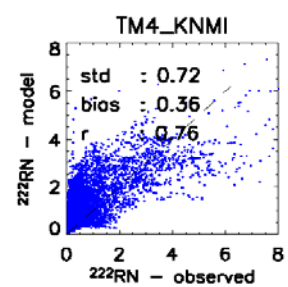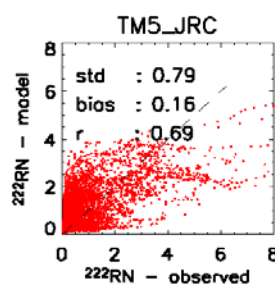
Figure 3.4: continued.
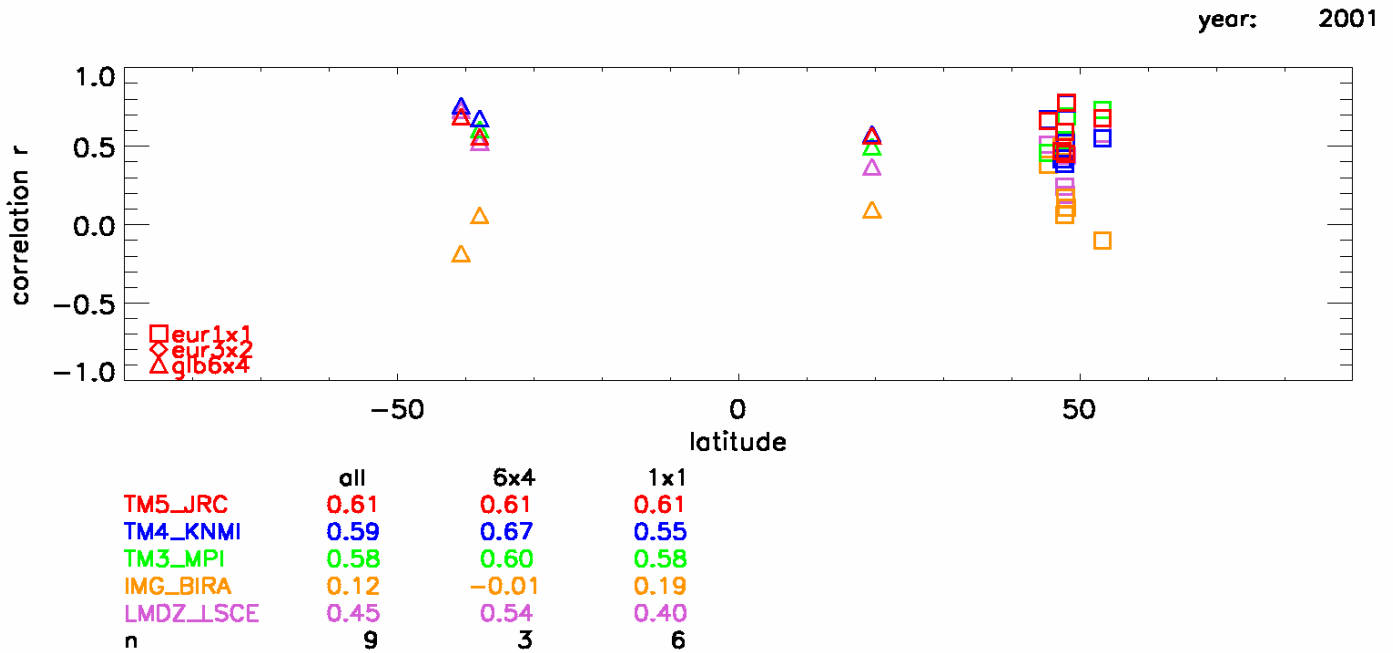
Figure 3.5: Correlation between observations and model simulations as function of latitude. Data points are separated for different TM5 domains (global 6°x4°, European 3°x2° , and European 1°x1°. Within the European 1°x1° higher correlation is achieved by the TM5 model compared to TM4 (with globally uniform resolution of 3°x2°), while outside the European zoom the TM4 achieves higher correlation (i.e. 3°x2° (TM4) vs. 6°x4° (TM5)).

4   SF$_6$ intercomparison

4.1   SF$_6$ Modelling protocol

SF$_6$ emissions
The EDGAR V3.2 SF$_6$ inventory for 1995 is used for the *whole* simulation period (1994-2001) (see Fig. 4.1).

SF$_6$ sink
the SF$_6$ sink is assumed to be zero.

Initialization and simulation period
simulation period: 2001 (1 full year, spin-up 1994-2000)
initialization: Initial fields of SF$_6$ have been provided by MPI Jena (S. Körner), based on TRANSCOM simulations and representing atmospheric mixing ratios at 01.01.1994.

4.2   SF$_6$ results

The 3D distributions of simulated SF$_6$ mixing ratios are illustrated in Fig. 4.2 (surface), Fig 4.3 (free troposphere at 500 hPa), and Fig 4.4 (vertical distribution). Surface mixing ratios are significantly elevated close to the main SF$_6$ emission regions of North America, Europe, and Southeast Asia. Consistent with the ^{222}Rn simulations, these enhancements are somewhat stronger in TM5 and TM4 than in the other 3 models.
Furthermore, significant differences in the NS gradients of SF$_6$ mixing ratios are visible. This gradient is weakest for the LMDZ model, indicating faster interhemispheric mixing than in other models.
We calculate the 3D interhemispheric exchange time T$_{NS}$ [*Denning et al.*, 1999] as:

$$T_{NS} = \frac{C_N - C_S}{\frac{d}{dt}(C_N - C_S) - \left(\frac{S_N}{M_N} - \frac{S_S}{M_S}\right)}$$ (eq 4.1)

where C, S, and M represent the (hemispheric) SF$_6$ mixing ratios, SF$_6$ emissions, and air masses, and the subscripts N and S refer to the northern and southern hemisphere. Monthly values of T$_{NS}$ are shown in Fig. 4.6, yearly mean values in Table 4.1. This compilation confirms that LMDZ has a much faster interhemispheric exchange time (6.3 months) than the other models (TM5, TM4, TM3: 9.9-10.4 months; IMAGES: 12.5 months). This overall range is similar to the range for the models of the TransCom2 intercomparison (6.6-15.1 months) [*Denning et al.*, 1999]. Fig 4.4 also shows large differences in the vertical SF$_6$ distribution, in particular in the upper troposphere and stratosphere, indicating significant differences in the stratospheric-tropospheric exchange time (T$_{STE}$). We calculate T$_{STE}$ as:

$$T_{STE} = \frac{C_T - C_S}{\frac{d}{dt}C_S}$$ (eq 4.2)

from the mixing ratios C in the troposphere (T) and stratosphere (S), and the stratospheric increase (and assuming a constant tropopause at 150 hPa). STE is weaker (15.1–16.6 months) in TM5, TM4, and LMDZ than in TM3 and IMAGES (7.9-8.7 months). The difference in STE between TM3 vs. TM5/TM4 is probably largely due to the different vertical resolution of the applied model versions.

Measurements of SF_6 by balloons [*Patra et al.*, 1997] and satellites [*Rinsland et al.*, 2005] showed typical gradients between the middle stratosphere and the troposphere in the order of 0.8 ppt (0.7-1.0 ppt). This is similar to the gradient simulated by TM5, TM4, and LMDZ (~0.8 ppt), while TM3 (~0.4 ppt) and IMAGES (~0.2 ppt) have much smaller gradients (Figure 4.4). Therefore, the greater T_{STE} of TM5, TM4, and LMDZ seems more realistic. However, a more detailed analysis will have to take into account the variation of the vertical stratospheric SF_6 gradient with latitude, and also with time.

Comparison of model simulations with surface measurements are shown in Fig. 4.5. The difference of model simulations between NH sites and SH sites (e.g. compare Barrow with South Pole) is reflecting the different T_{NS} (Table 4.1) of the models, leading to the smallest gradient between these two stations for the LMDZ model. It should be emphasized, however, that the surface mixing ratios (in particular in the NH) are also significantly influenced by the vertical mixing (see also [*Denning et al.*, 1999] for comparison of 1D, 2D, and 3D based calculations of T_{NS}).

Furthermore, it is interesting to note that at most background sites synoptic variations of SF_6 are very small, or not present at all (consistent between observations and simulations). An exception is station Schauinsland where significantly elevated SF_6 mixing ratios are observed during certain synoptic conditions. These are very well captured by the TM5, TM4 and TM3 model (with correlation coefficients of 0.41-0.51).

Table 4.1: Derived interhemispheric exchange time (T_{NS}) and stratospheric-tropospheric exchange time (T_{STE})

model	TM5 (JRC)	TM4 (KNMI)	TM3 (MPI)	IMAGES (BIRA-IASB)	LMDZ (CNRS-LSCE) external partner
T_{NS} [months]	10.4	9.9	10.0	12.5	6.3
T_{STE} [months]	16.6	16.3	8.7	7.9	15.1

total

EDGARV3.0
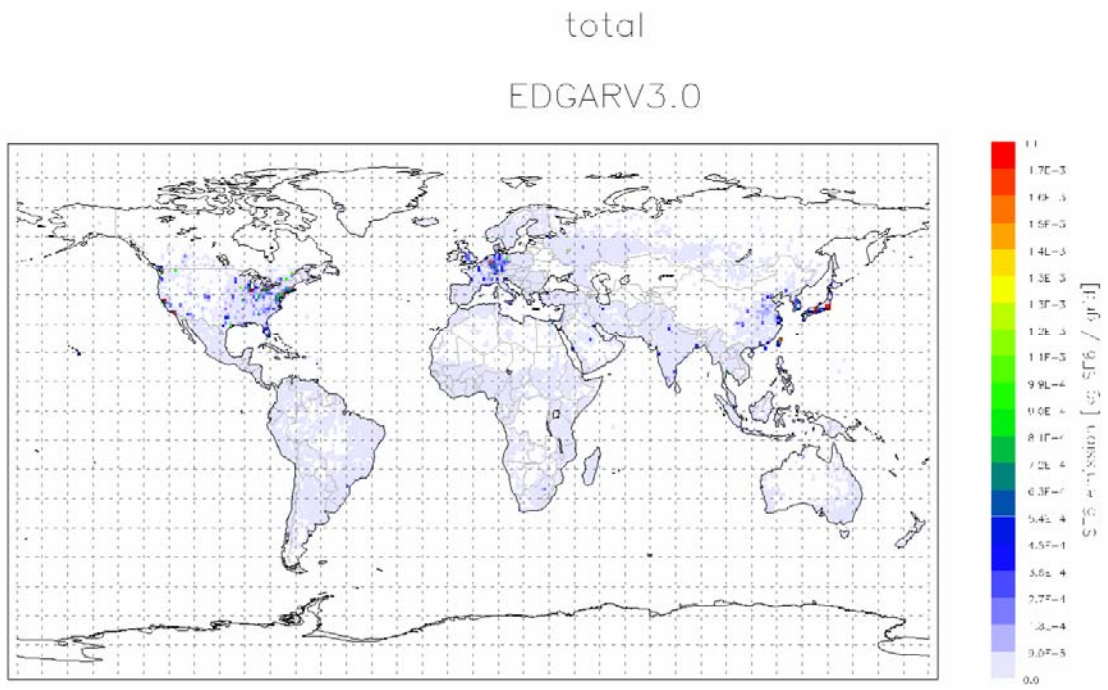
Figure 4.1: SF$_6$ emissions

surface June
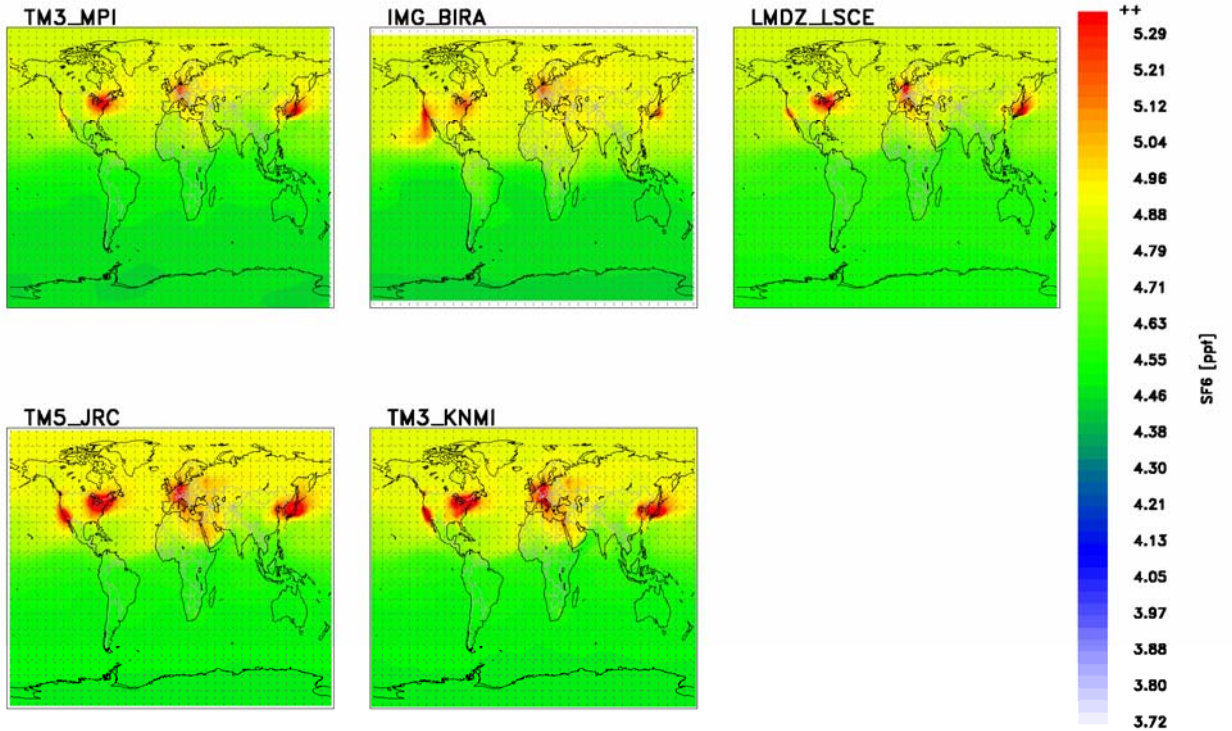
surface December
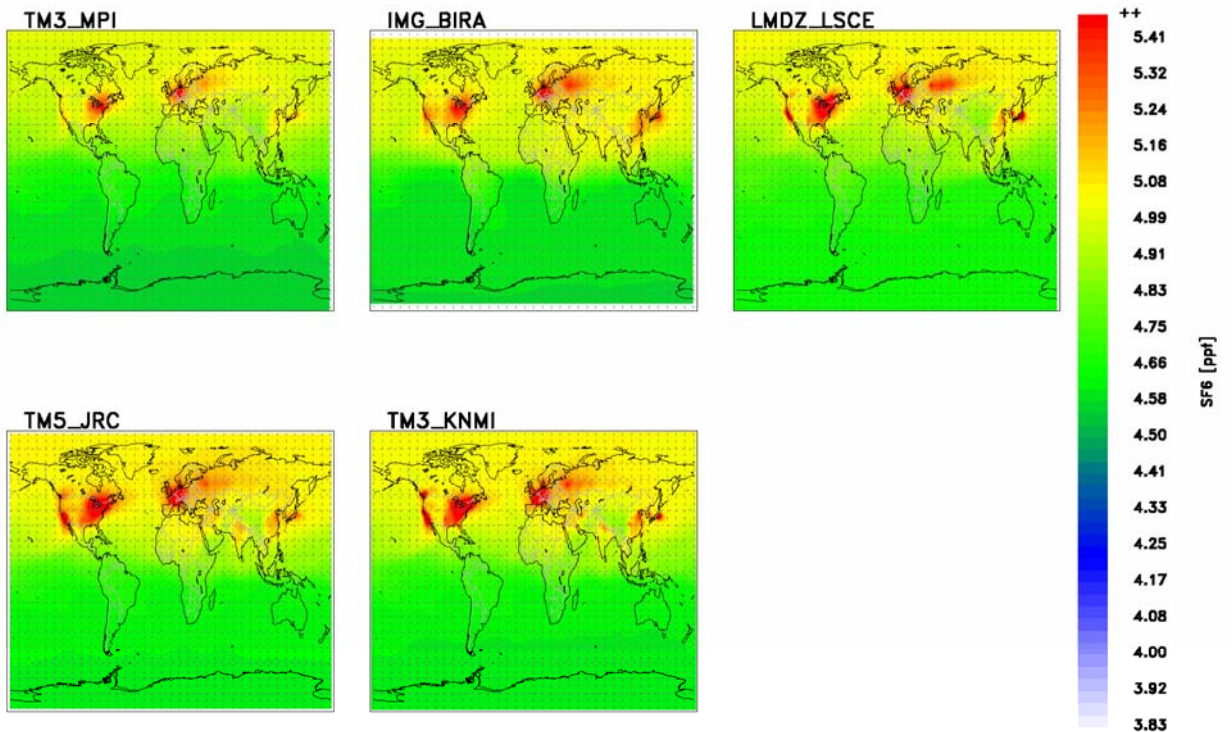
Figure 4.2: SF$_6$ intercomparison: surface (top: June 2001; bottom: December 2001). Note change in color scale (to account for atmospheric increase).
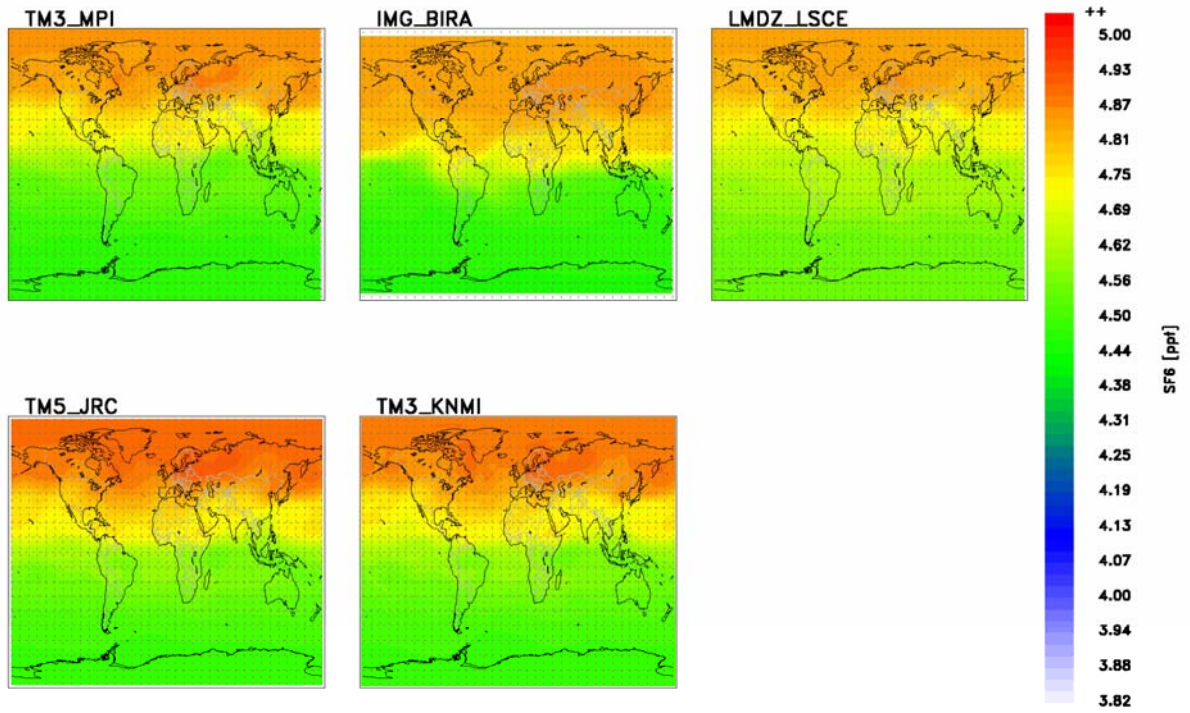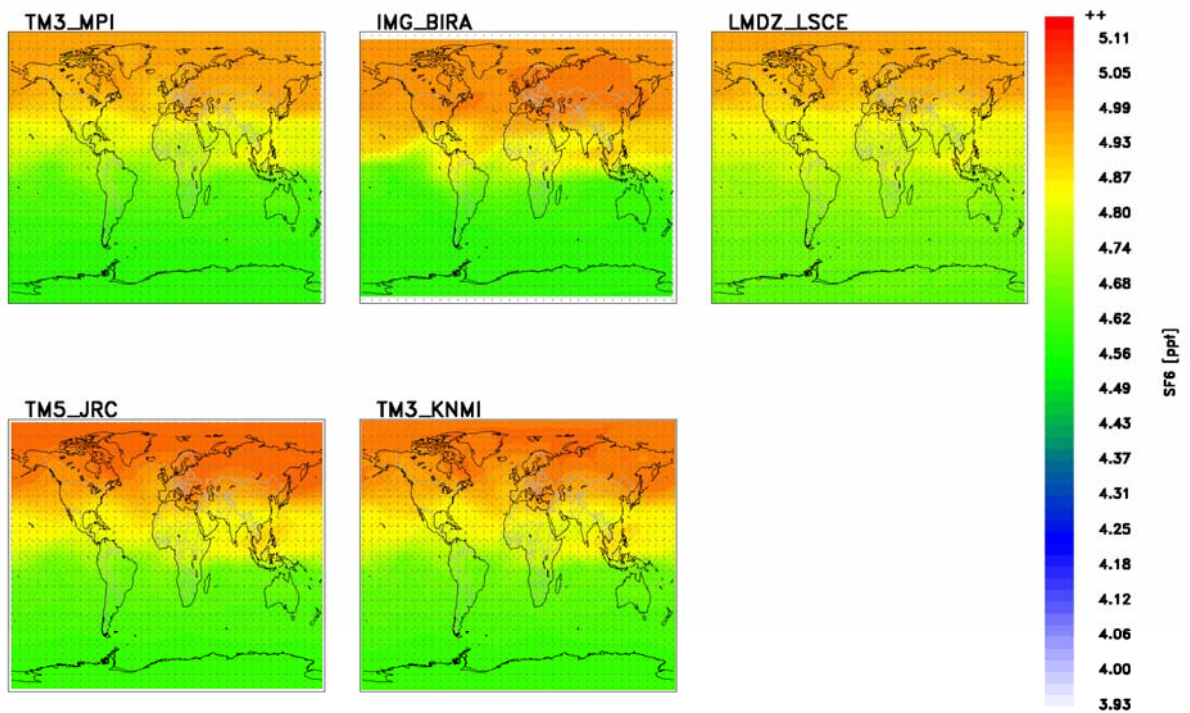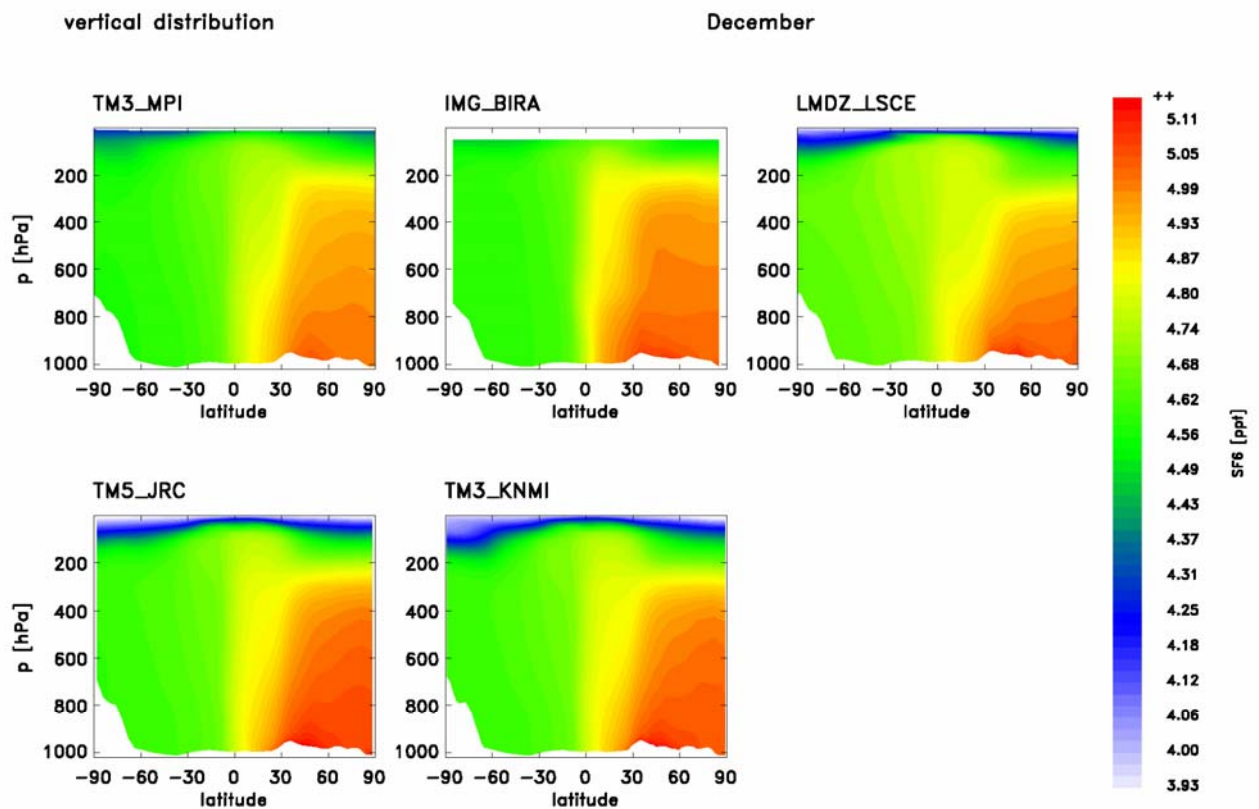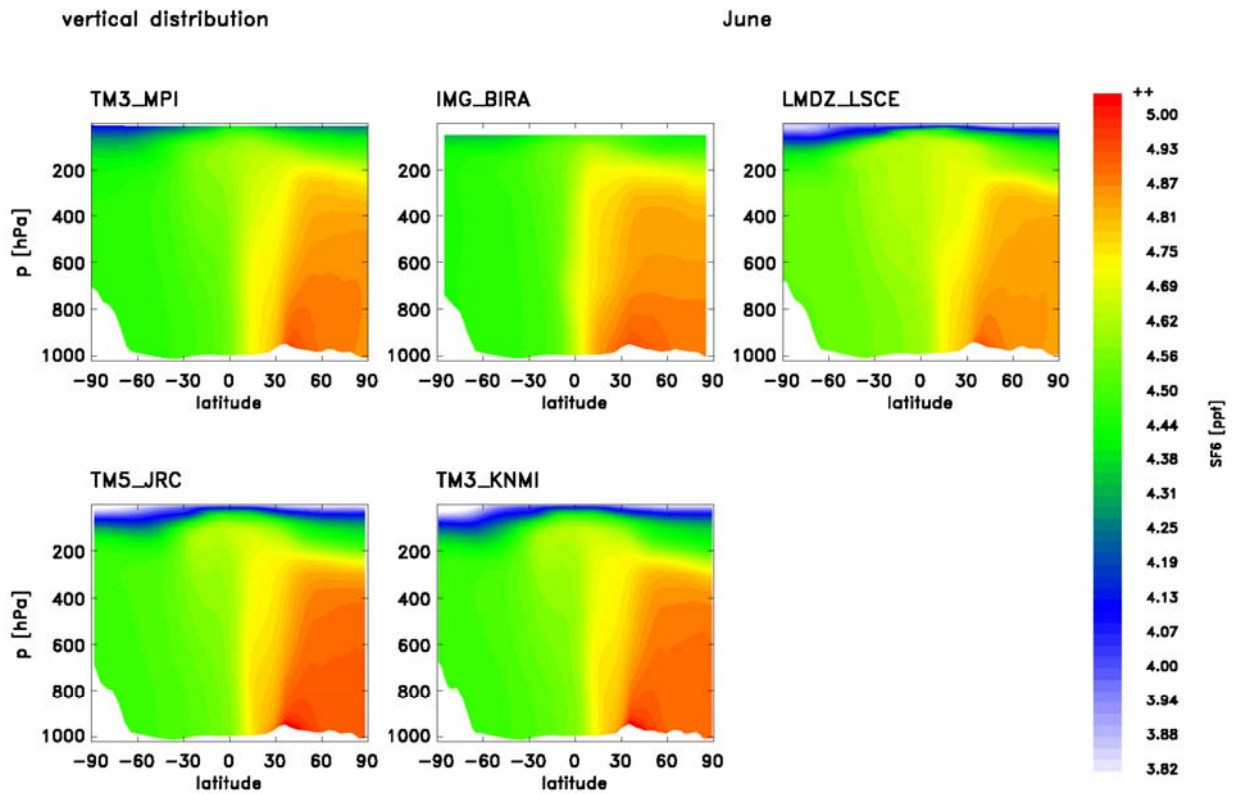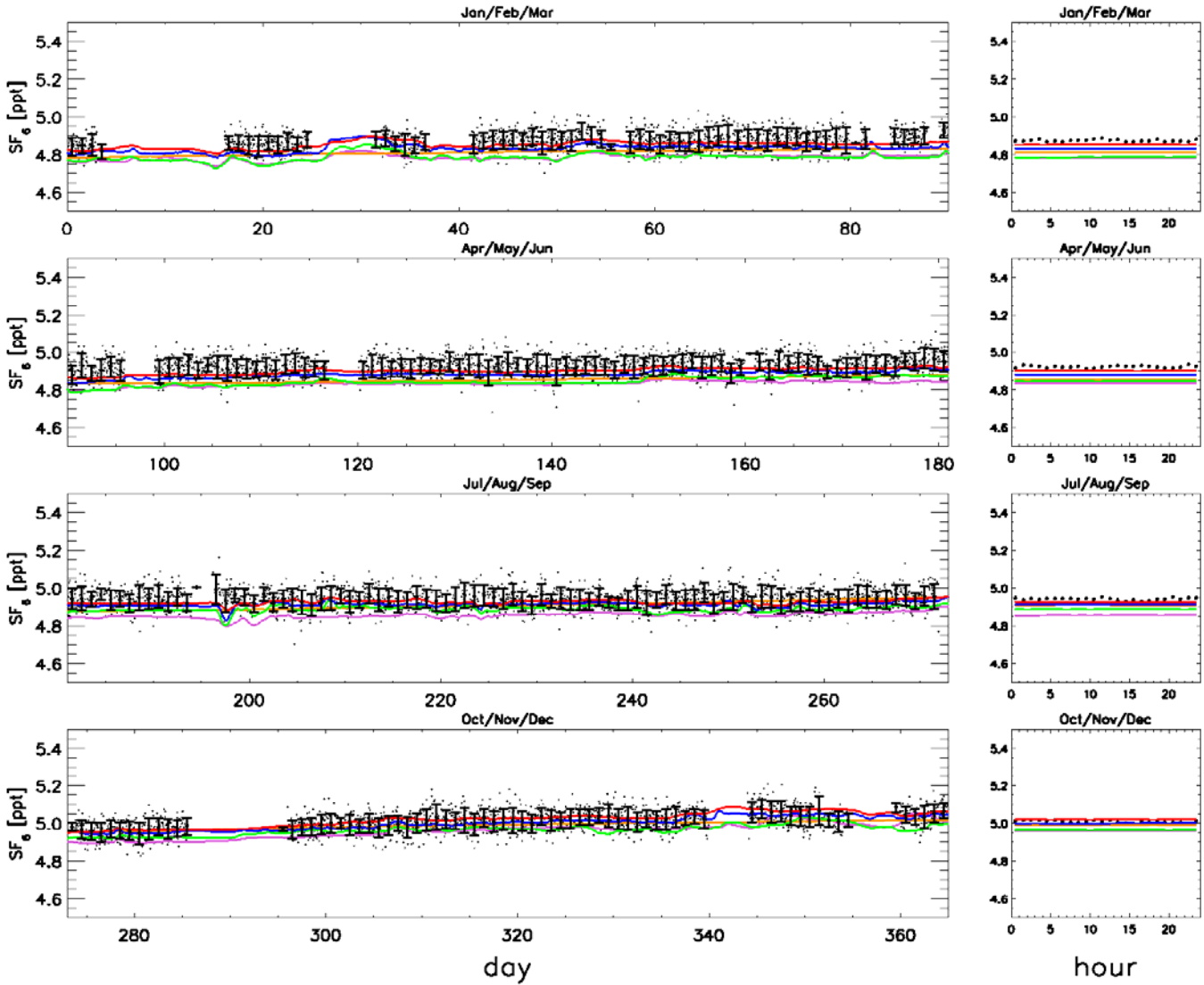
Figure 4.3: SF$_6$ intercomparison: free troposphere (500 hPa) (top: June 2001; bottom: December 2001). Note change in color scale (to account for atmospheric increase).

vertical distribution   June

vertical distribution   December

[6] intercomparison: vertical distribution (latitudinal averages) (top: June 2001; bottom: December 2001). Note change in color scale (to account for atmospheric increase).
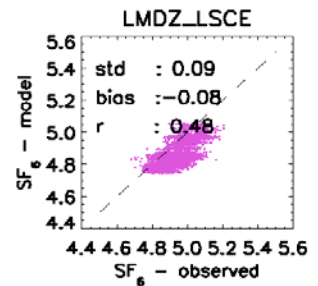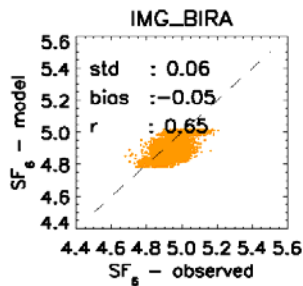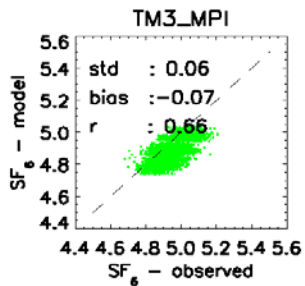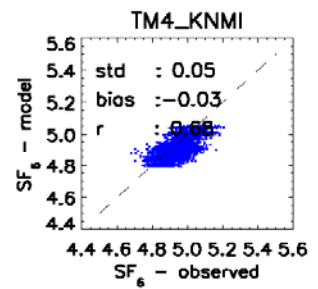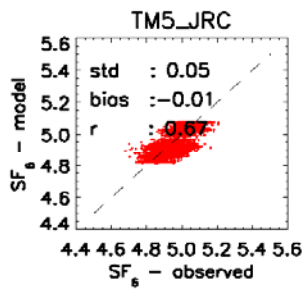
Figure 4.5: SF_6 intercomparison: Surface monitoring stations.

Figure 4.5: continued.

Figure 4.5: continued.

MLO_WDC(19.53 N,-155.58 E, 3397.0 m asl) Mauna Loa, USA   2001
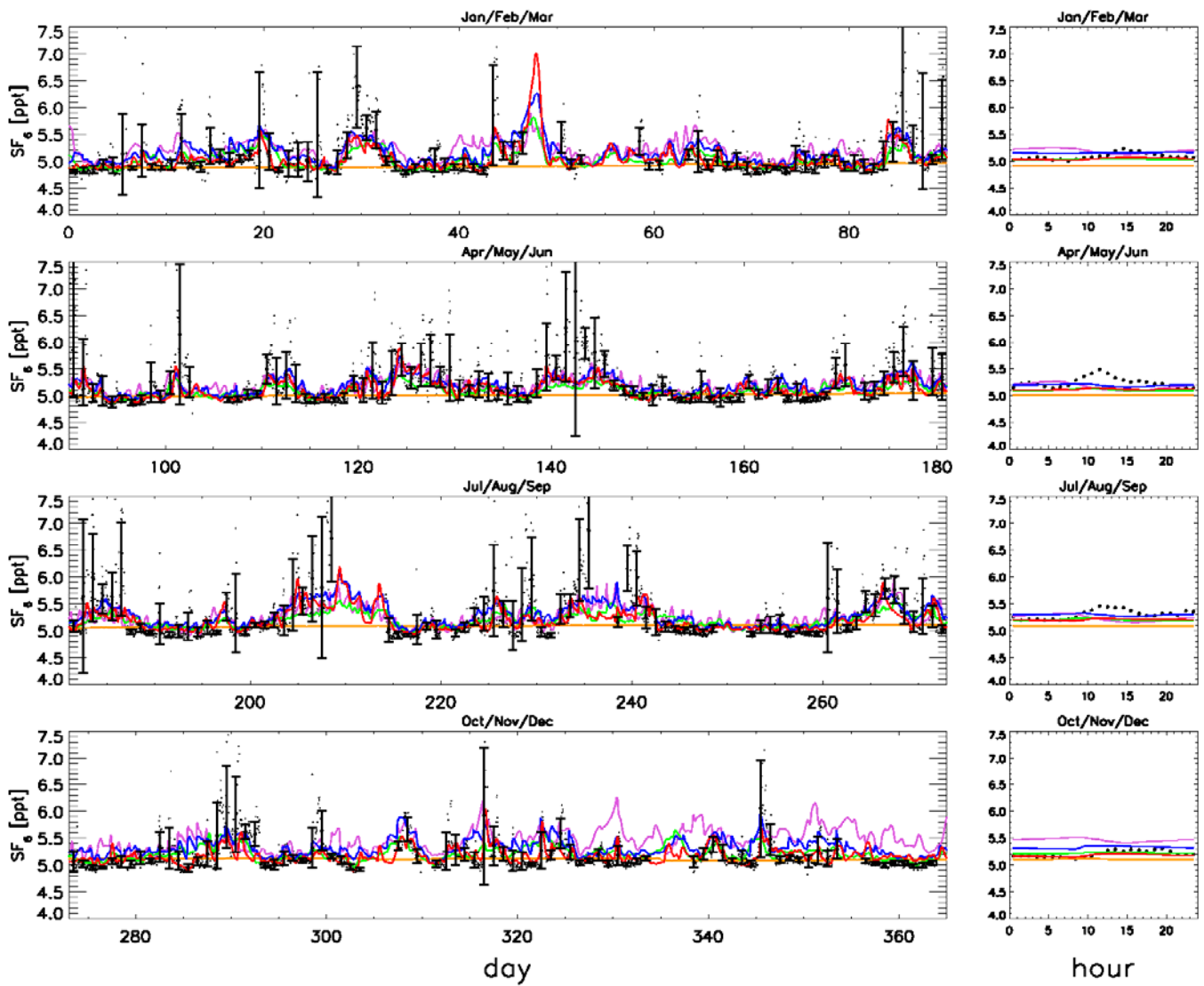
TM5_JRC
TM4_KNMI
TM3_MPI
IMG_BIRA
LMDZ_LSCE

Figure 4.5: continued.

SMO_WDC(−14.25 N,−170.57 E, 42.0 m asl) Tutuila, Samoa, USA 2001

Figure 4.5: continued.

SPO_WDC(−89.98 N, −24.80 E, 2810.0 m asl) South Pole, Antarctica   2001

TM5_JRC
TM4_KNMI
TM3_MPI
IMG_BIRA
LMDZ_LSCE

TM5_JRC
std : 0.13
bias :−0.14
r   : 0.43

TM4_KNMI
std : 0.13
bias :−0.13
r   : 0.43

TM3_MPI
std : 0.12
bias :−0.15
r   : 0.44

IMG_BIRA
std : 0.12
bias :−0.16
r   : 0.44

LMDZ_LSCE
std : 0.12
bias :−0.08
r   : 0.43

Figure 4.5: continued.

30

Figure 4.6: SF$_6$ intercomparison: SF$_6$ intercomparison: Upper panel: Interhemispheric exchange time T$_{NS}$ (eq. 4.1); lower panel: stratospheric-tropospheric exchange time T$_{STE}$ (eq. 4.2).

5   CH$_4$ intercomparison

5.1   CH$_4$ Modelling protocol

CH$_4$ emissions
CH$_4$ emission were taken from [*Bergamaschi et al.*, 2005] (a priori emissions for year 2001; see Fig. 5.1).

CH$_4$ sink
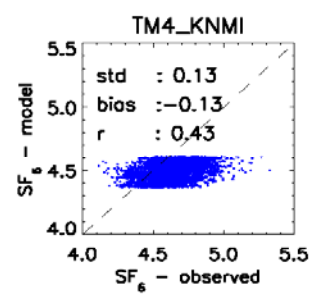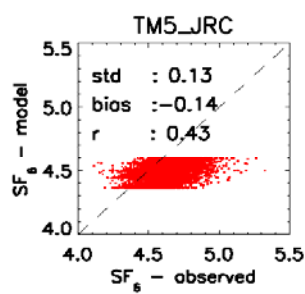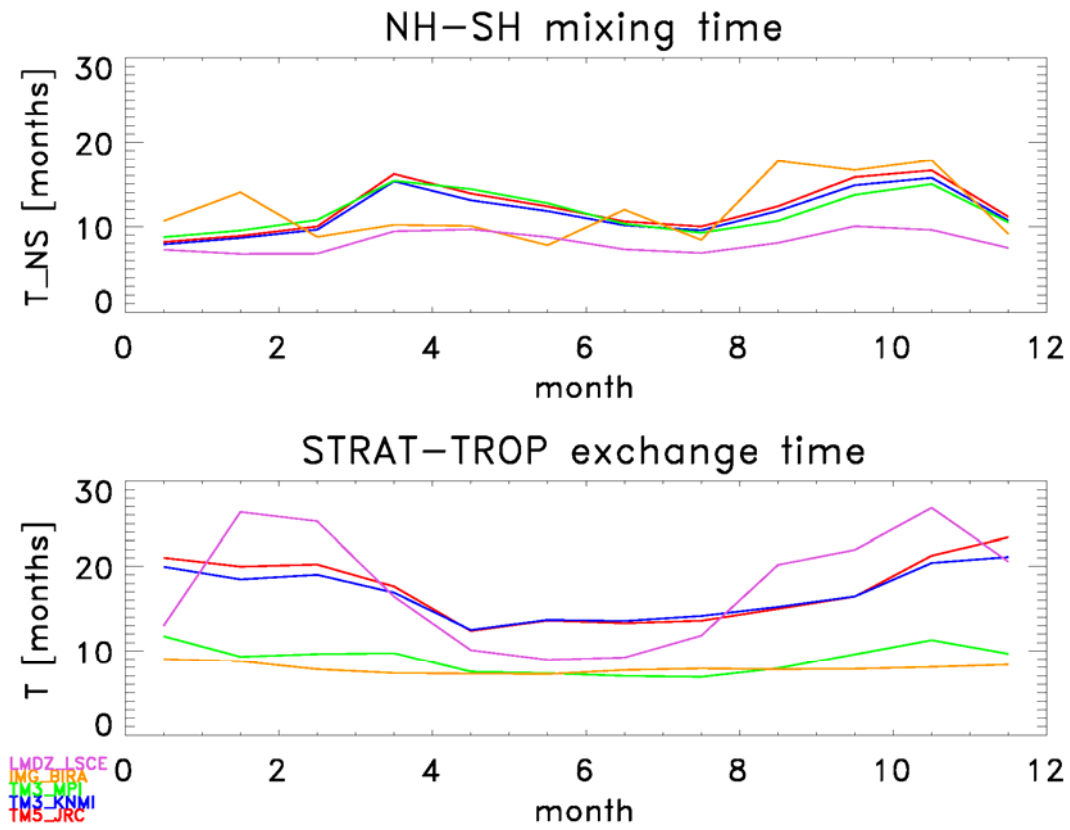CH$_4$ + OH sink was used as described in [*Bergamaschi et al.*, 2005]. This OH distribution is also illustrated in section 6 ("TM5_JRC_offline"). In the stratosphere, also CH$_4$ destruction by O(1D), Cl is taken into account [*Bergamaschi et al.*, 2005; *Brühl and Crutzen*, 1993].

Initialization and simulation period
simulation period: 2001-2003 (3 full years + spin-up 1 year), i.e.
model start: 01/01/2000
model end: 31/12/2003
initialization: Initial fields of CH$_4$ (for 01.01.2000) have been provided by JRC (P. Bergamaschi)

5.2   CH$_4$ results

CH$_4$ simulations were performed with the TM5, TM4 and IMAGES model. Despite the prescribed CH$_4$ sinks, the different 3D distibutions of CH$_4$ in the models lead to a small drift in CH$_4$ mixing ratios of IMAGES vs. TM5/TM4 of about 20 ppb within 3 years. To facilitate comparison of plots with have subtracted this offset of 20 ppb for the IMAGES results in all plots (for year 2003).
The 3D distributions of simulated CH$_4$ mixing ratios are illustrated in Fig. 5.2 (surface), Fig 5.3 (free troposphere at 500 hPa), and Fig 5.4 (vertical distribution). The CH$_4$ distribution reflects the major differences between the models as seen from the ^{222}Rn and SF$_6$ simulations:

- TM5 and TM4 have higher surface CH$_4$ mixing ratios than IMAGES over CH$_4$ source regions (due to the weaker vertical mixing).
- TM5 and TM4 have a slightly smaller inter-hemispheric gradient than IMAGES due to the somewhat higher inter-hemispheric exchange (i.e. smaller T_{NS}).
- TM5 and TM4 have a much more pronounced vertical gradient in the upper troposphere and stratosphere due to the significantly higher T_{STE}.
- TM5 and TM4 simulations are very similar (confirming the consistency between the two models) but also show the effect of the different horizontal resolution (resolution 3°x2^o (TM4) vs. 6°x4^o (TM5)), in particular over source regions.

Fig. 5.5 shows comparison with flask measurements from the NOAA network, and Fig. 5.6 comparison with continuous measurements from different networks (NOAA, AGAGE, UBA). TM5 and TM4 generally simulate the synoptic variability rather well

and achieve overall very good correlations with observations (r=0.57-0.59; Fig. 5.7).
As for ^{222}Rn a clear improvement is visible with increasing model resolution.
On the global domain TM4 achieves higher correlation with measurements than TM5
(resolution $3^{o}x2^{o}$ (TM4) vs. $6^{o}x4^{o}$ (TM5)), on the European zoom domain the
correlation for TM5 is higher ($1^{o}x1^{o}$ (TM5) vs. $3^{o}x2^{o}$ (TM4)).
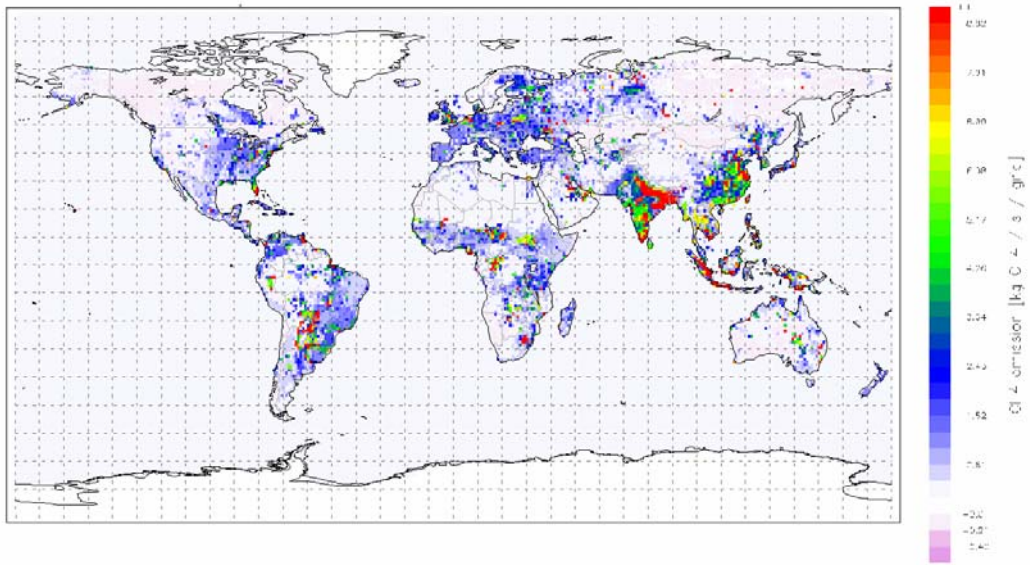
Figure 5.1: CH$_4$ emissions

surface   June

TM4_KNMI   TM5_JRC

IMG_BIRA

surface   December
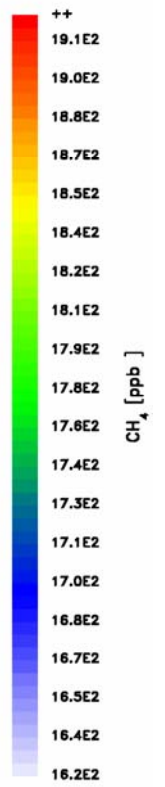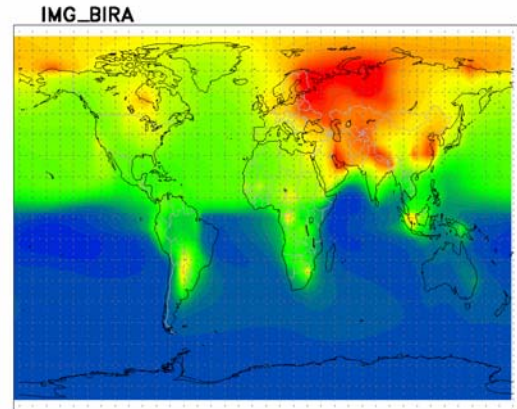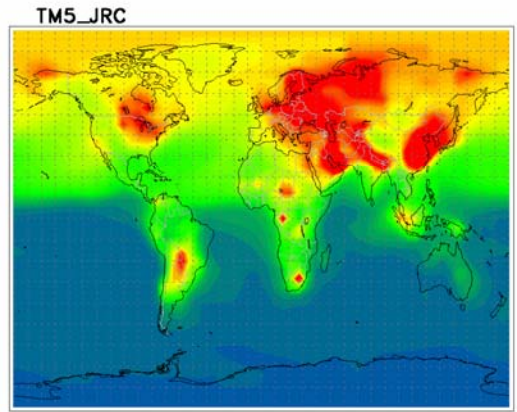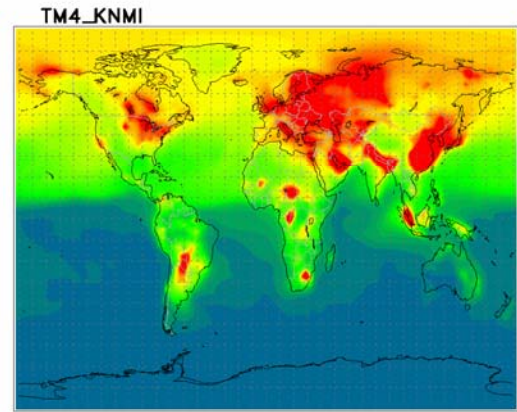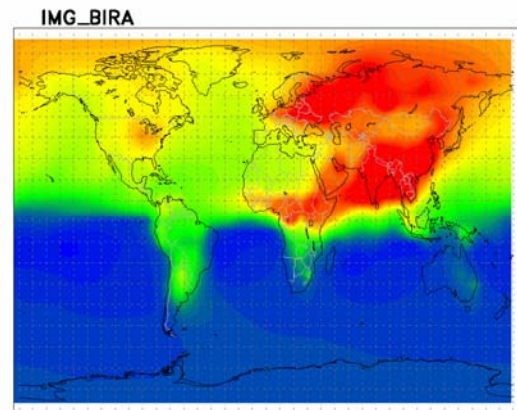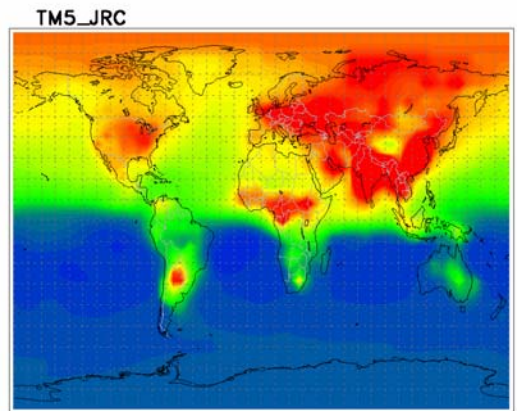
TM4_KNMI   TM5_JRC
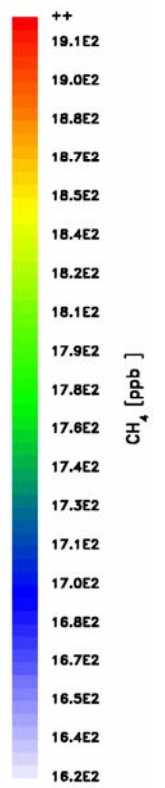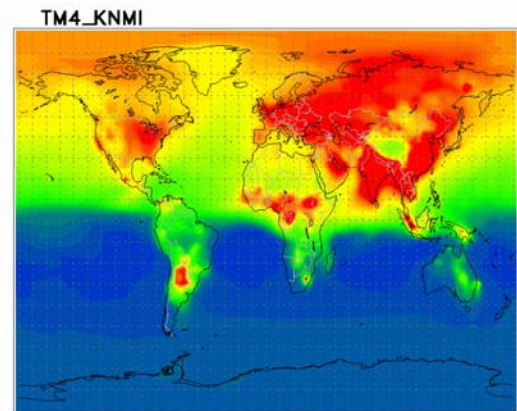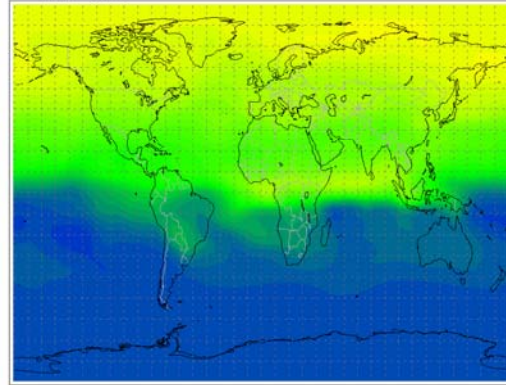
IMG_BIRA
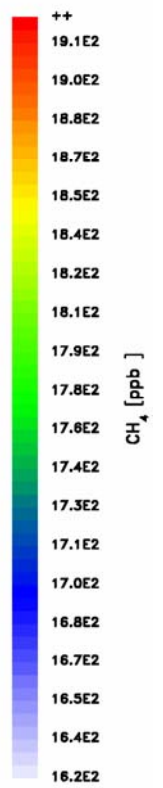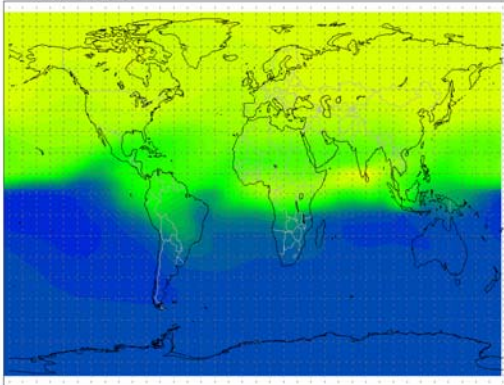
Figure 5.2: CH$_4$ intercomparison: surface (top: June 2003; bottom: December 2003).

Figure 3.9. CH_4 intercomparison: free troposphere (500 hPa) (top: June 2003; bottom: December 2003).
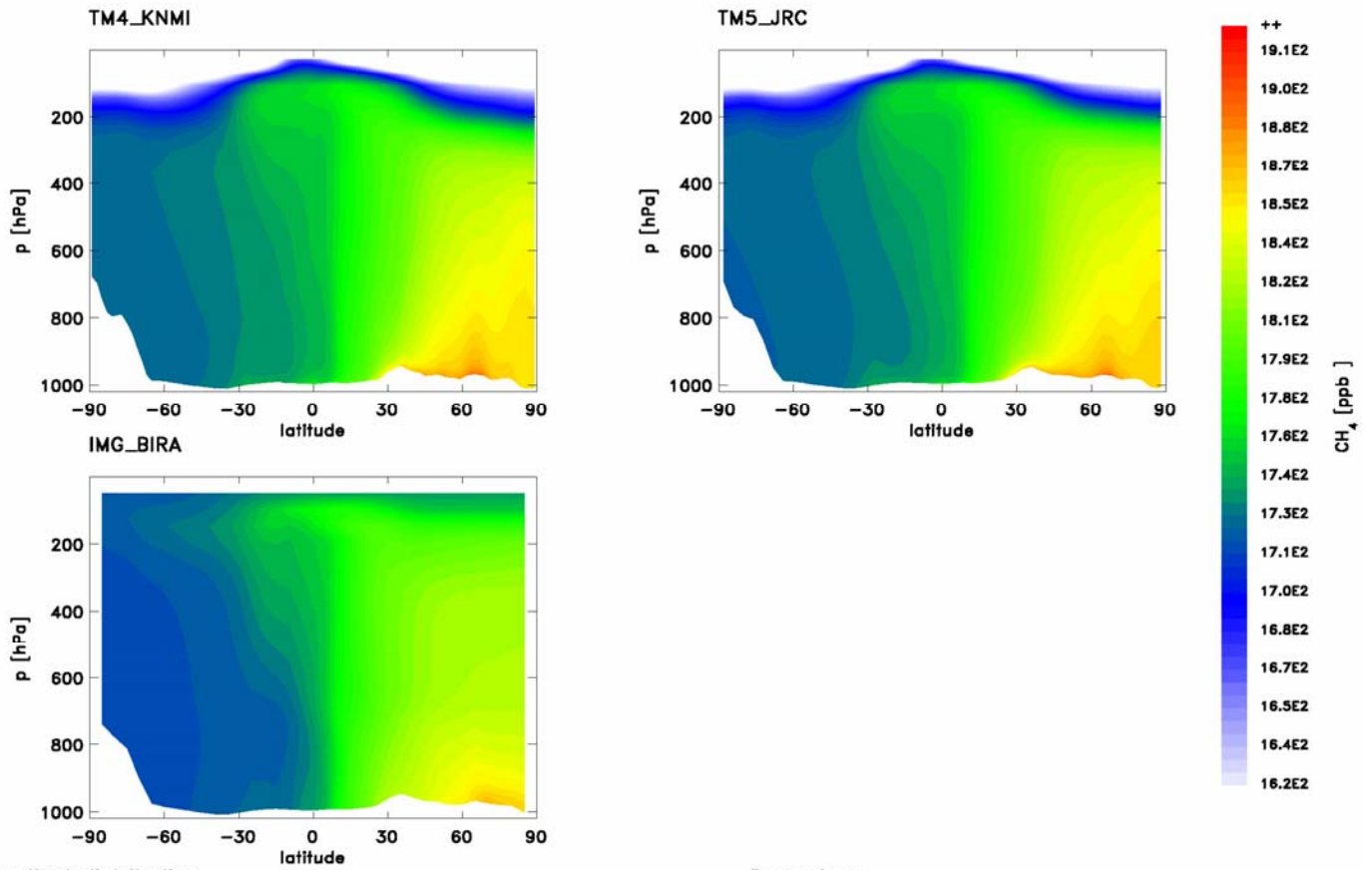
Figure 5.4: CH$_4$ intercomparison: vertical distribution (latitudinal averages) (top: June 2003; bottom: December 2003).
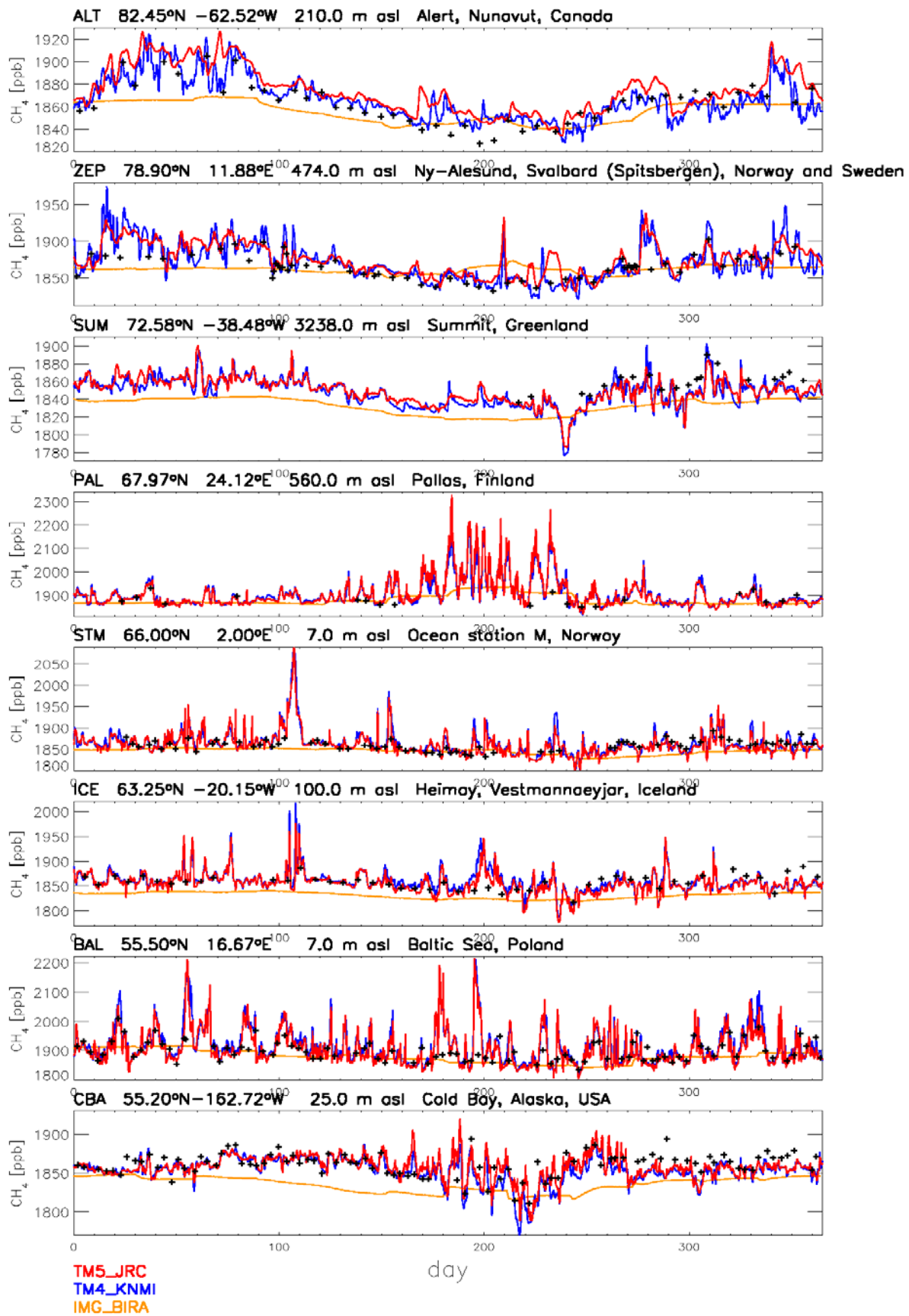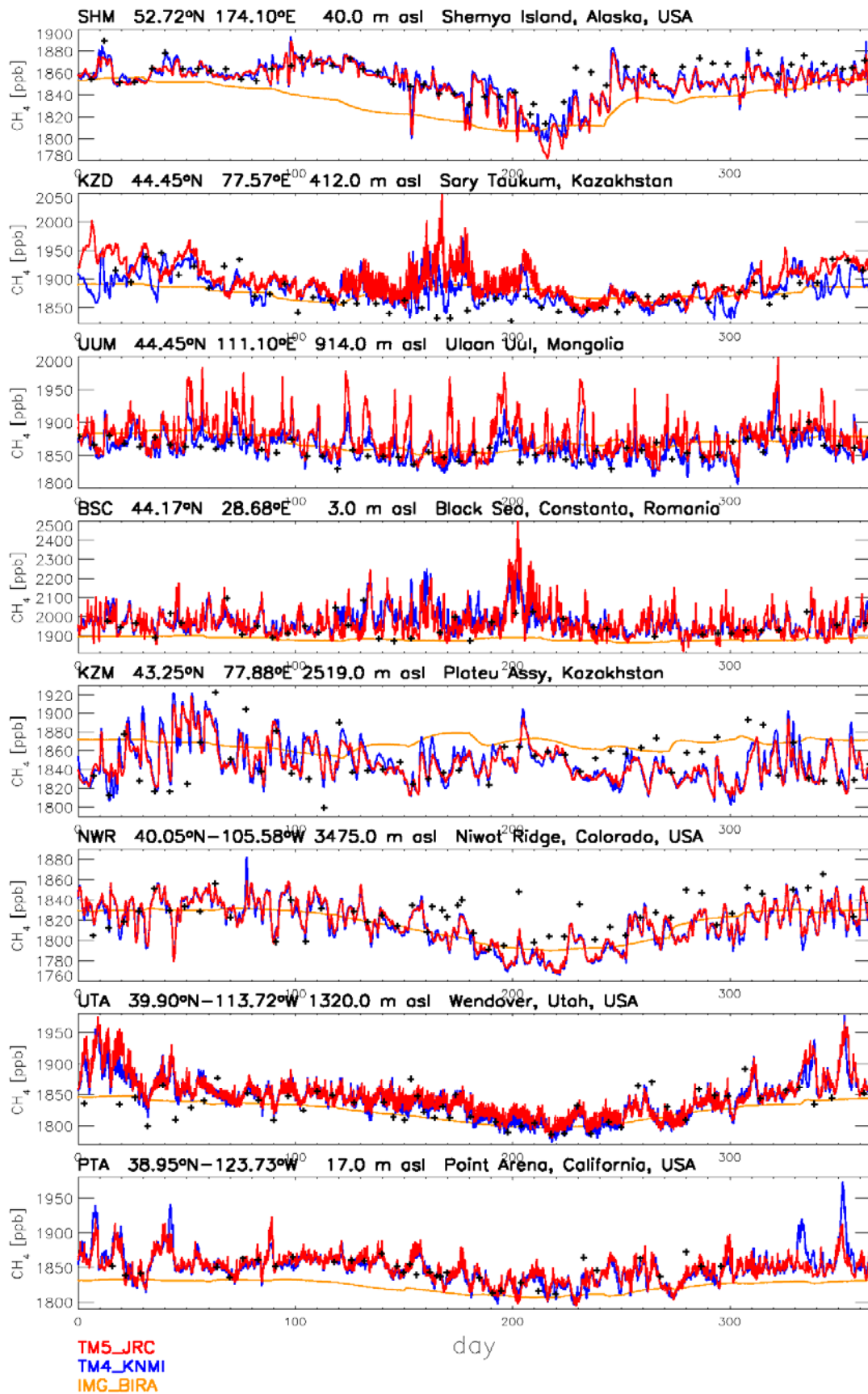
Figure 5.5: continued.
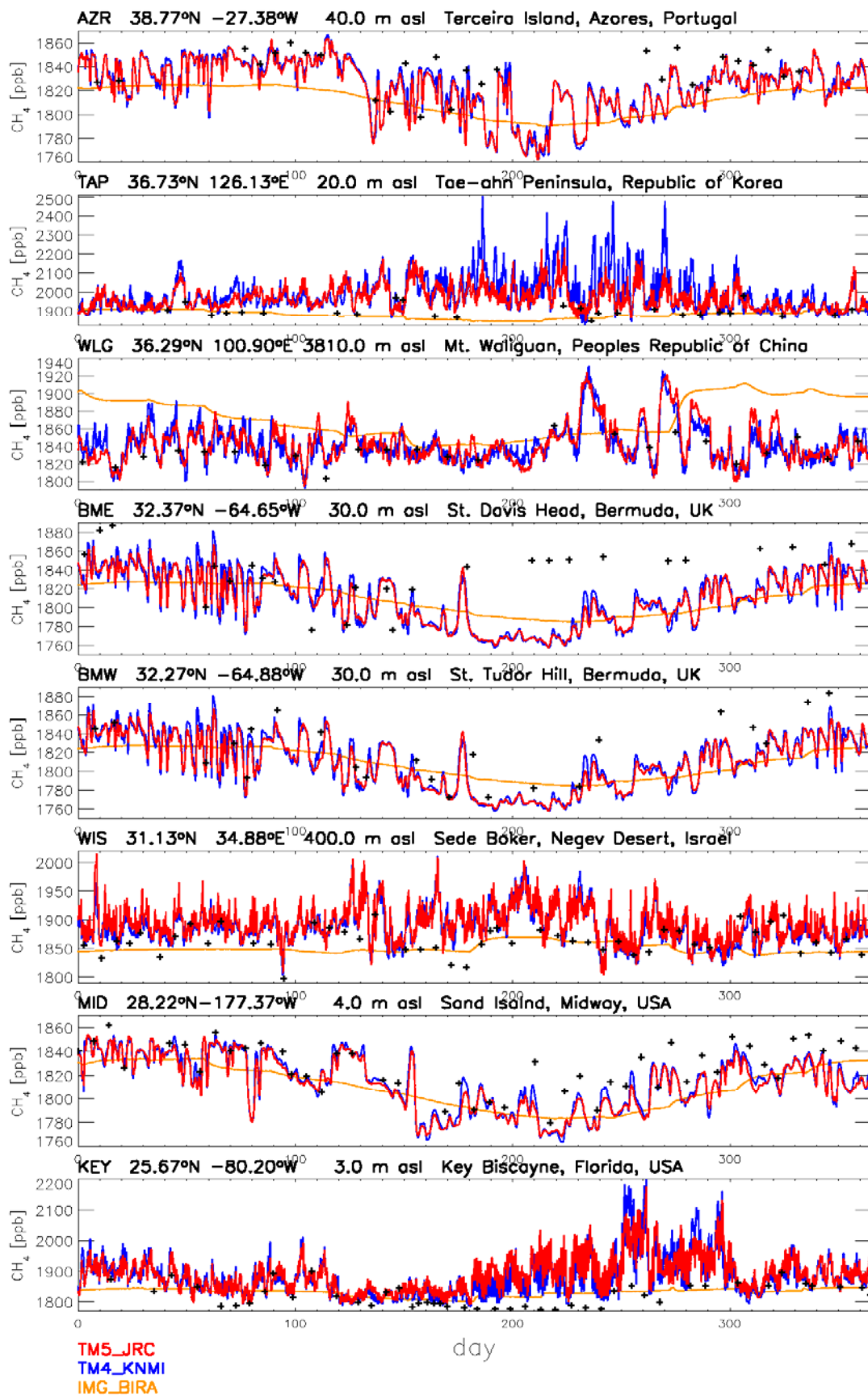
Figure 5.5: continued.
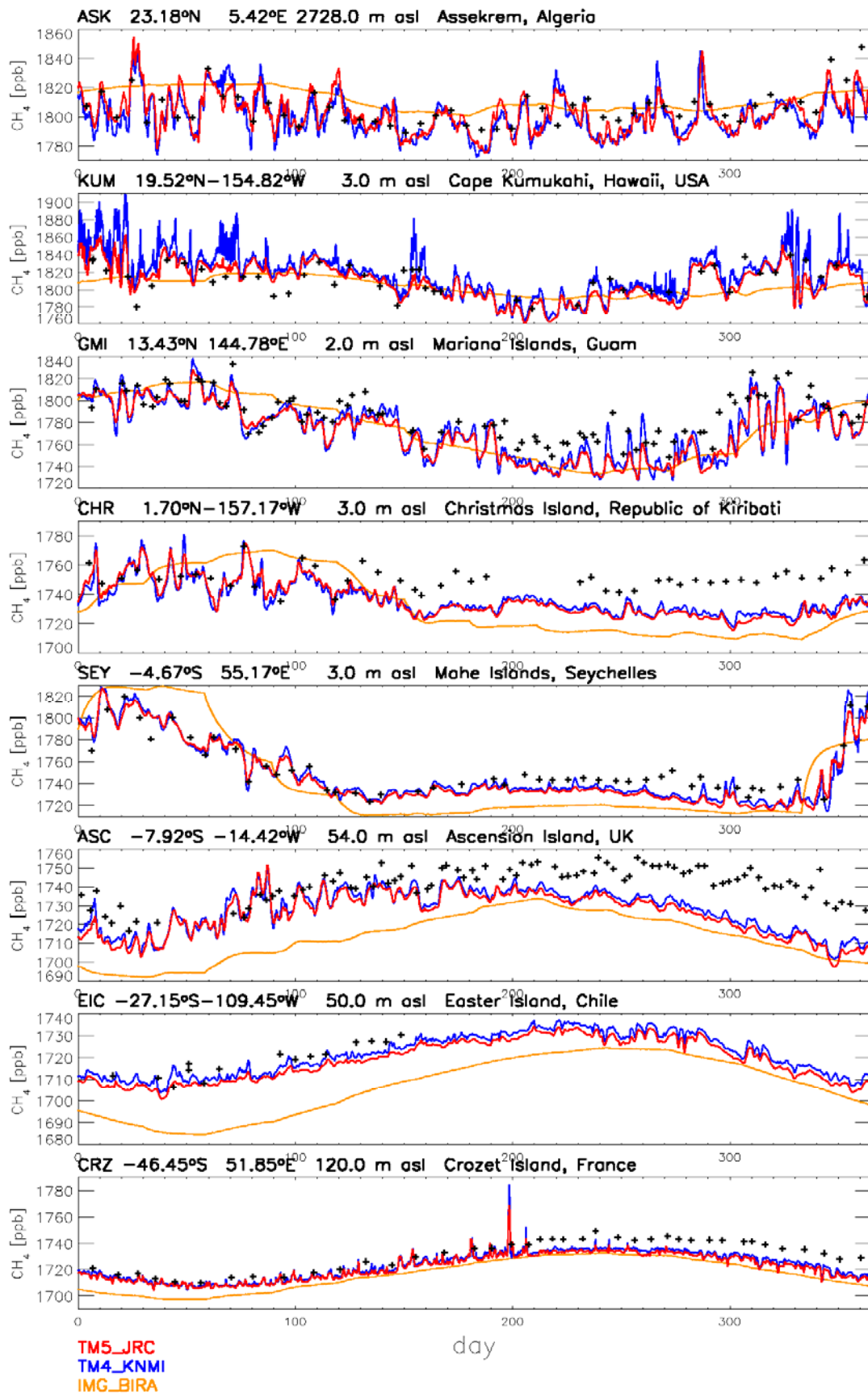
Figure 5.5: continued.
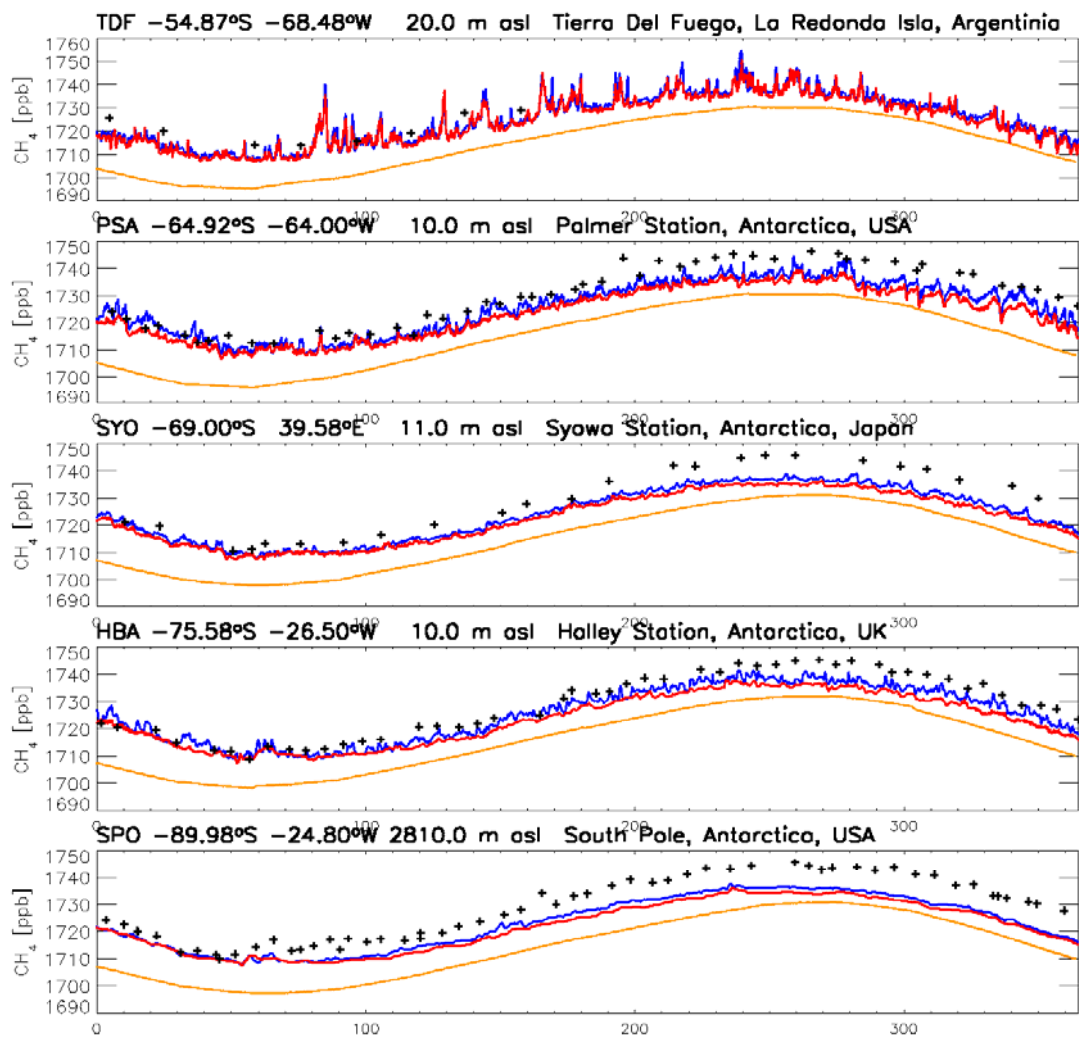
Figure 5.5: continued.
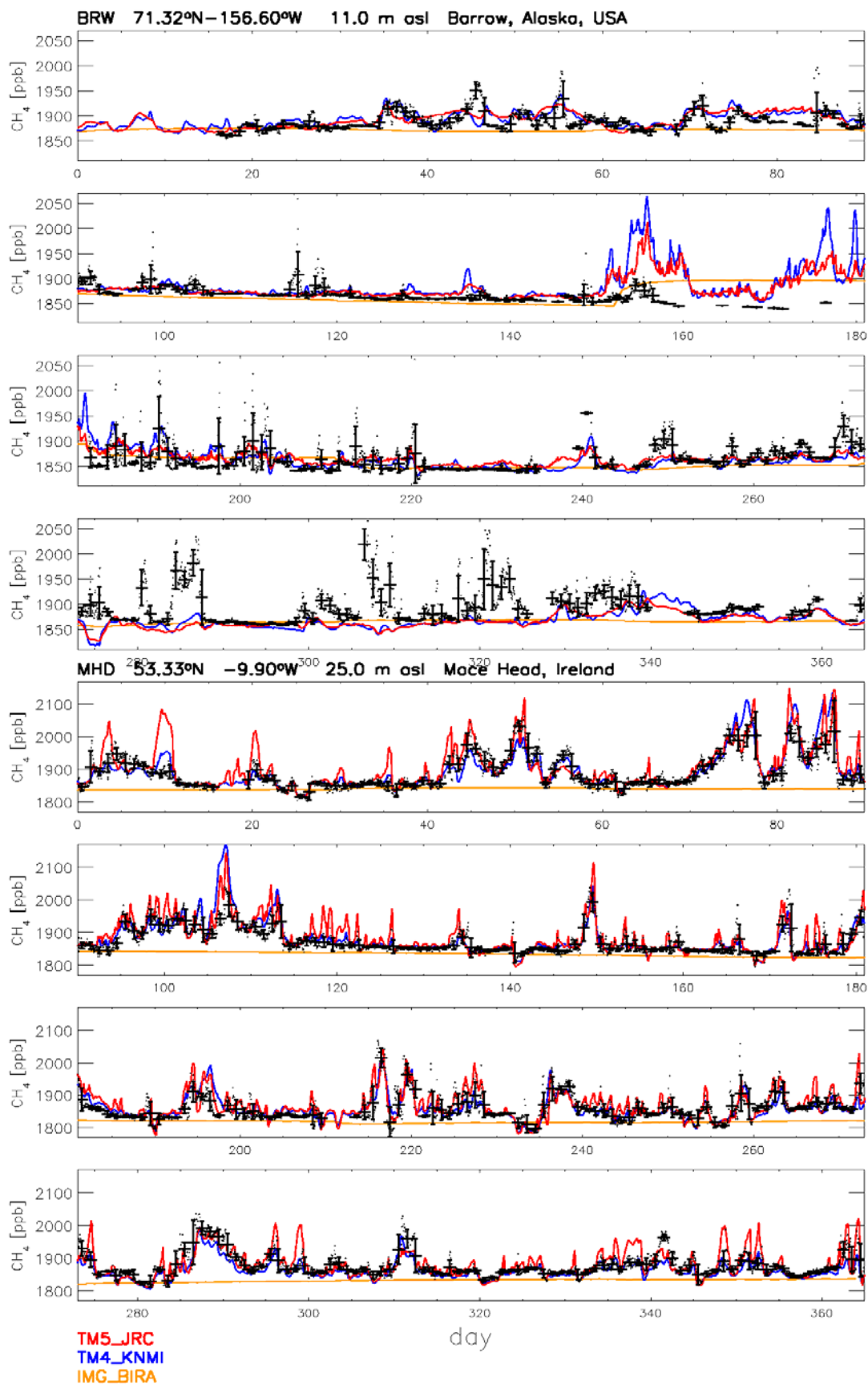
Figure 5.6: CH$_4$ intercomparison: surface monitoring sites: high frequency measurements from various networks (NOAA, AGAGE, UBA).

43
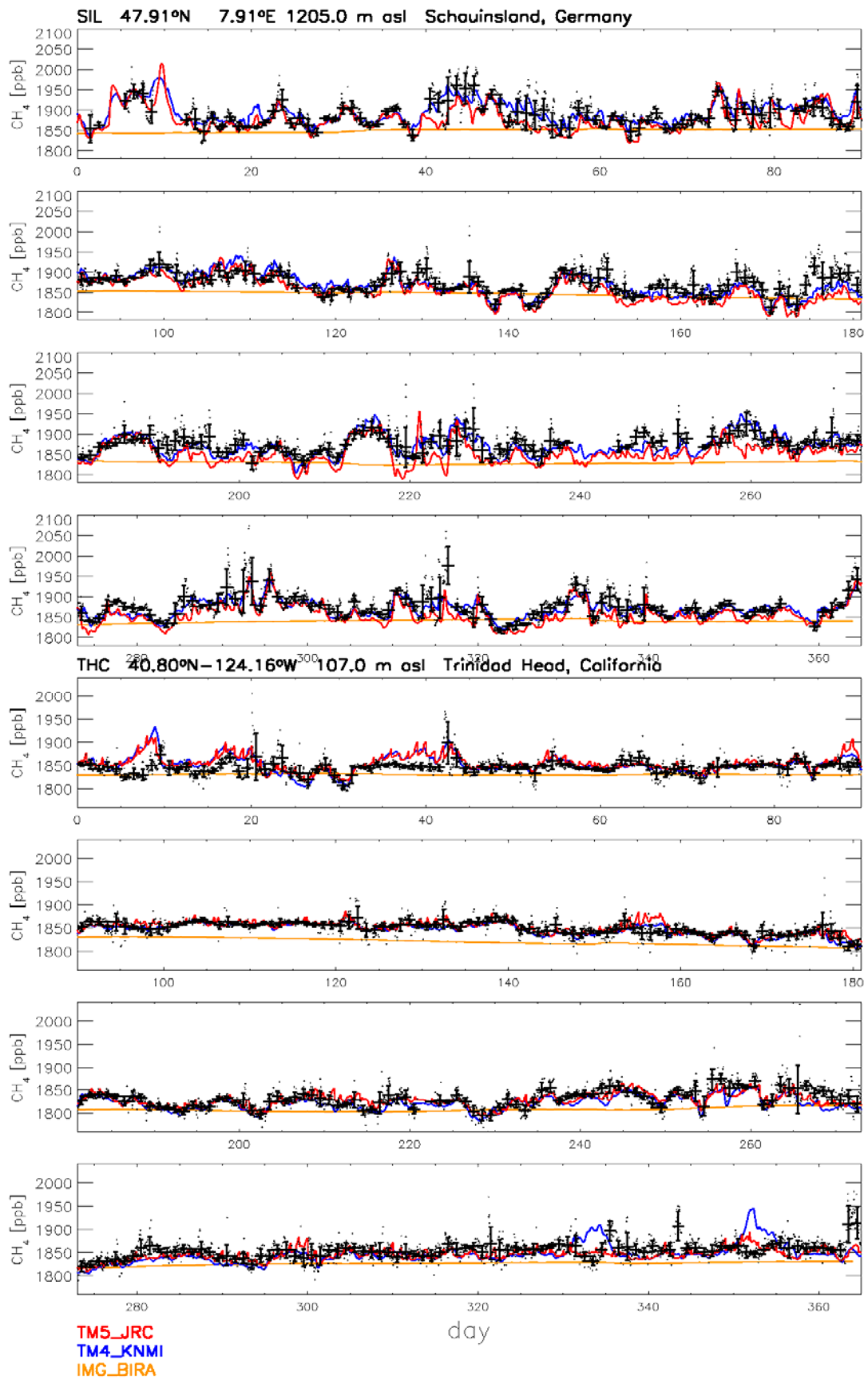
Figure 5.6: continued.
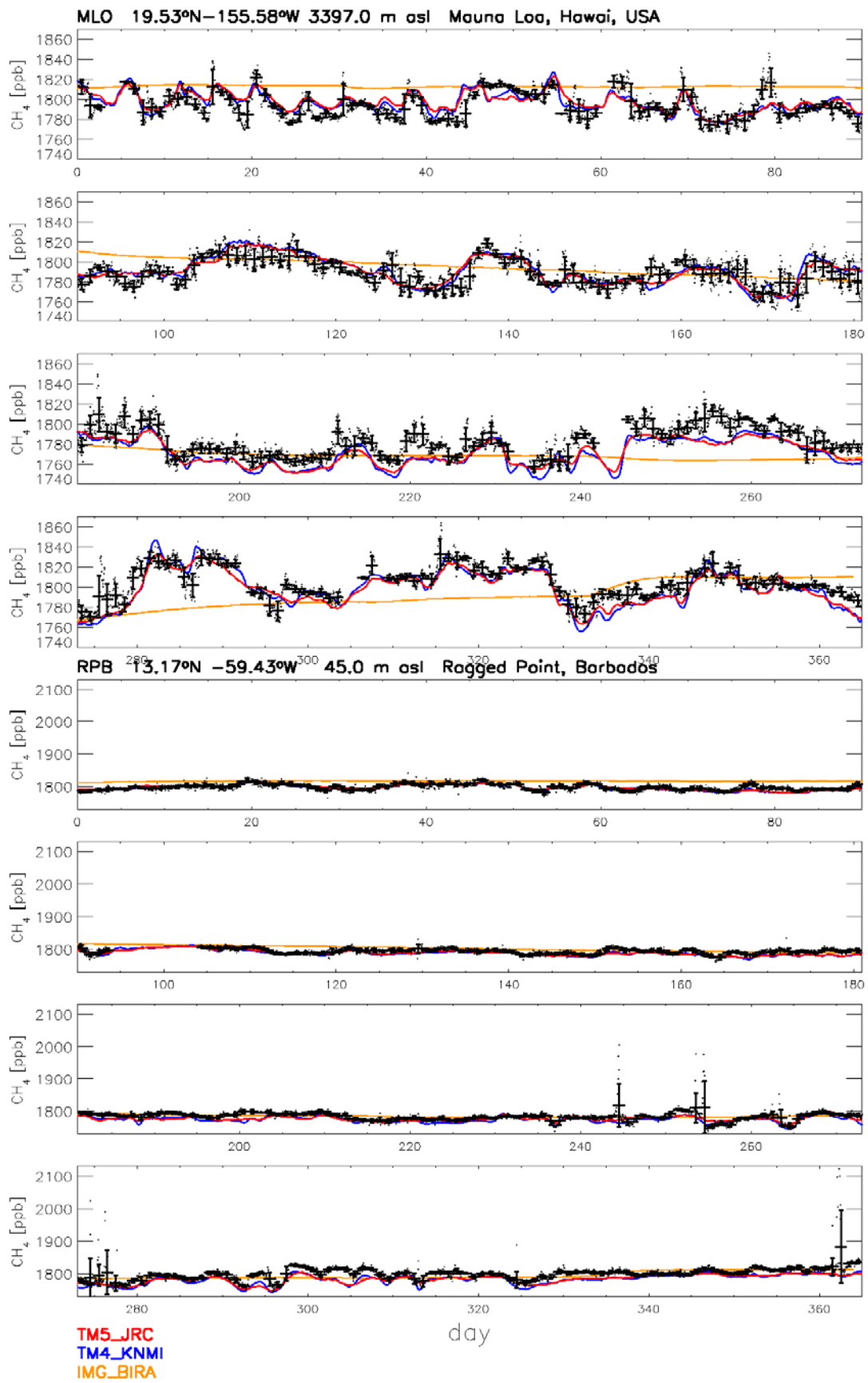
Figure 5.6: continued.
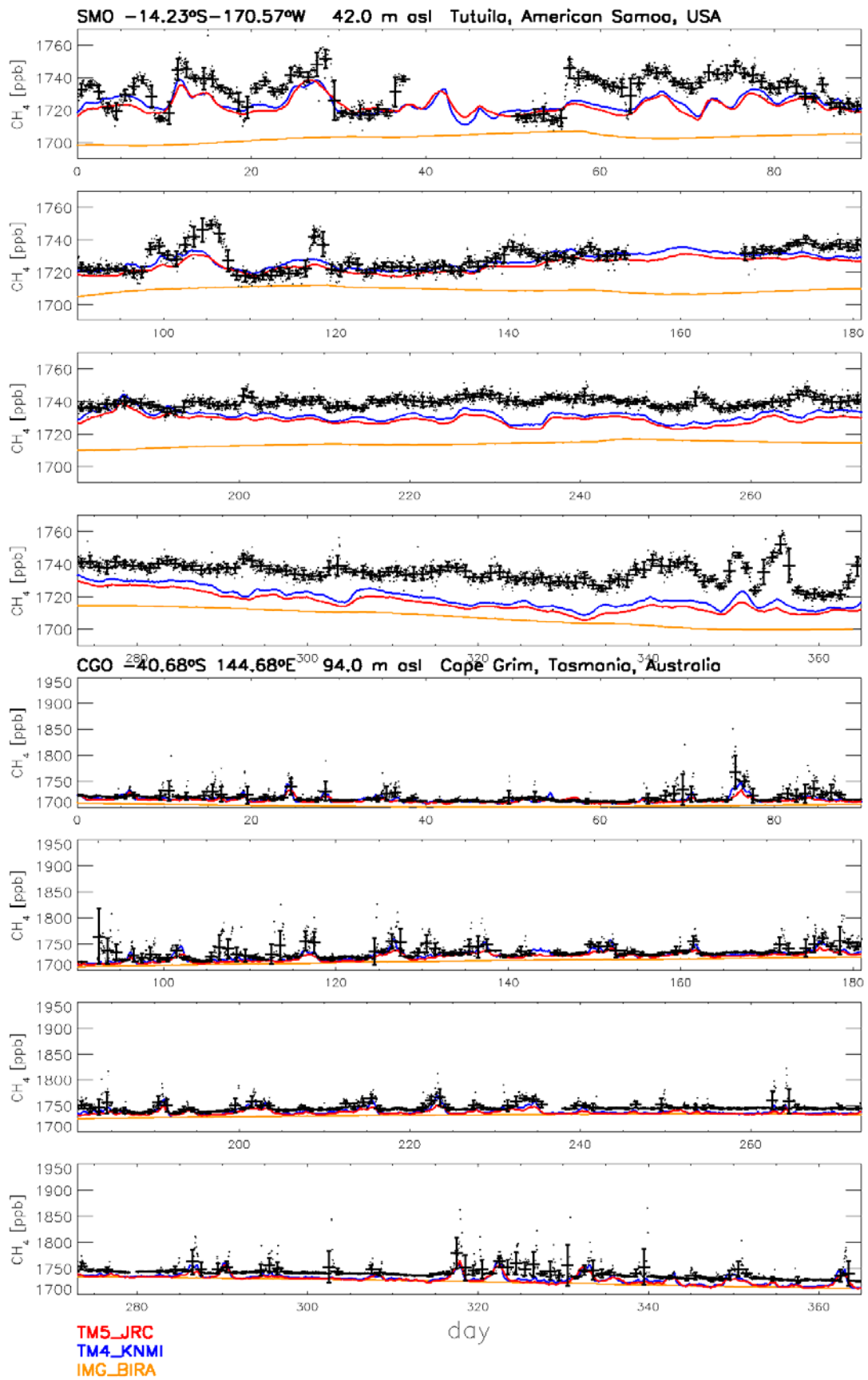
Figure 5.6: continued.
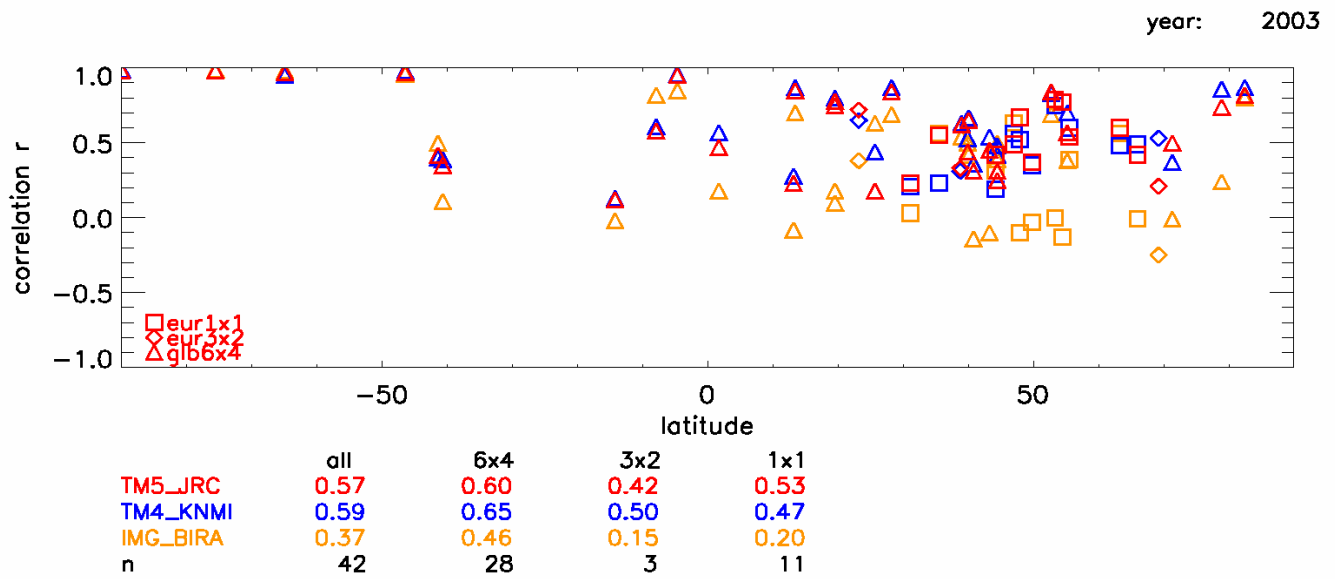
Figure 5.7: Correlation between observations and model simulations as function of latitude. Data points are separated for different TM5 domains (global $6^o\times4^o$, European $3^o\times2^o$, and European $1^o\times1^o$. Within the European $1^o\times1^o$ higher correlation is achieved by the TM5 model compared to TM4 (with globally uniform resolution of $3^o\times2^o$), while outside the European zoom the TM4 achieves higher correlation (i.e. $3^o\times2^o$ (TM4) vs. $6^o\times4^o$ (TM5)).

6 OH intercomparison

6.1 OH Modelling protocol

For this comparison, no specific modelling protocol was defined. Instead models have been applied in their typical configuration. Simulation period was year 2001.

6.2 OH results

The 3D distributions of simulated OH concentrations are illustrated in Fig. 6.1 (surface), Fig 6.2 (free troposphere at 500 hPa), and Fig 6.3 (vertical distribution). The OH distribution named "TM5_JRC_offline" has been used for the CH_4 intercomparison (section 5) and has been used in recent CH_4 inversion studies [*Bergamaschi et al.*, 2006; *Bergamaschi et al.*, 2005]. It has been calibrated with methyl cloroform, resulting in a mean tropospheric CH_4 lifetime vs. OH of 9.4 years, very close to the TAR recommended value of 9.6 years [*IPCC*, 2001]. For all other OH fields, no calibration has been performed. The resulting CH_4+OH lifetimes (turnover time for whole atmospher) are compiled in Table 6.1 and are in the range of 8.3 - 11.4 years. All models suggest 20-40% higher CH_4 lifetime in the SH, compared to the NH.
Simulated OH fields show significant differences near the surface (Fig. 6.1), probably largely due to the applied different emission inventories (CO, NMHC, NO_x). In the free troposphere, however, the spatial OH distribution are relatively similar (Fig. 6.2 and 6.3). Furthermore, the seasonal OH variation is very consistent for all model runs.

Table 6.1: Derived CH4+OH lifetimes for the whole atmosphere (i.e. troposphere + stratosphere) and both hemispheres, T_{NH+SH}, for the individual hemispheres (T_{NH}, T_{SH}) and ratio of lifetimes for both hemispheres (T_{SH}/T_{NH})

model	IMAGES (BIRA-IASB)	TM4 (KNMI)	TM5 (JRC)	TM5_offline (JRC)
T_{NH+SH}	9.9	11.4	8.3	10.2[1]
T_{NH}	8.5	10.6	7.7	9.4
T_{SH}	12.1	12.2	9.0	11.2
T_{SH}/T_{NH}	1.4	1.2	1.2	1.2

[1] tropospheric CH_4+OH lifetime: 9.4 years
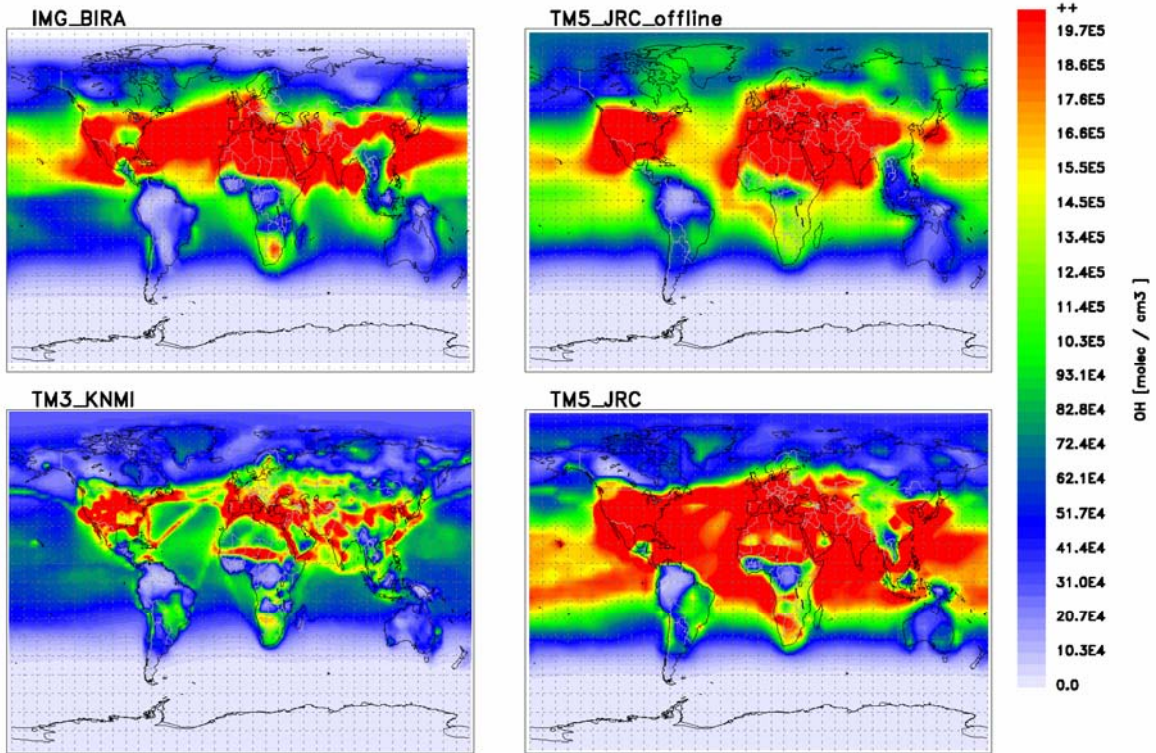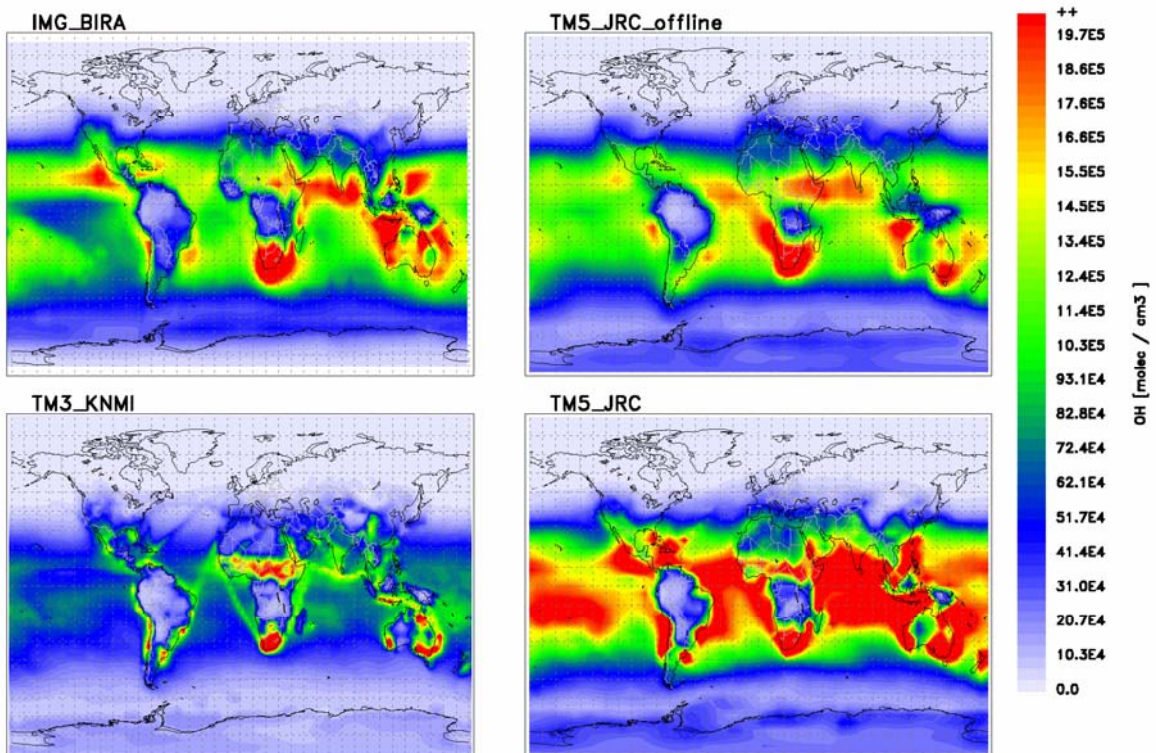
Figure 6.1: OH intercomparison: surface (top: June; bottom: December).

500.000hPa   June
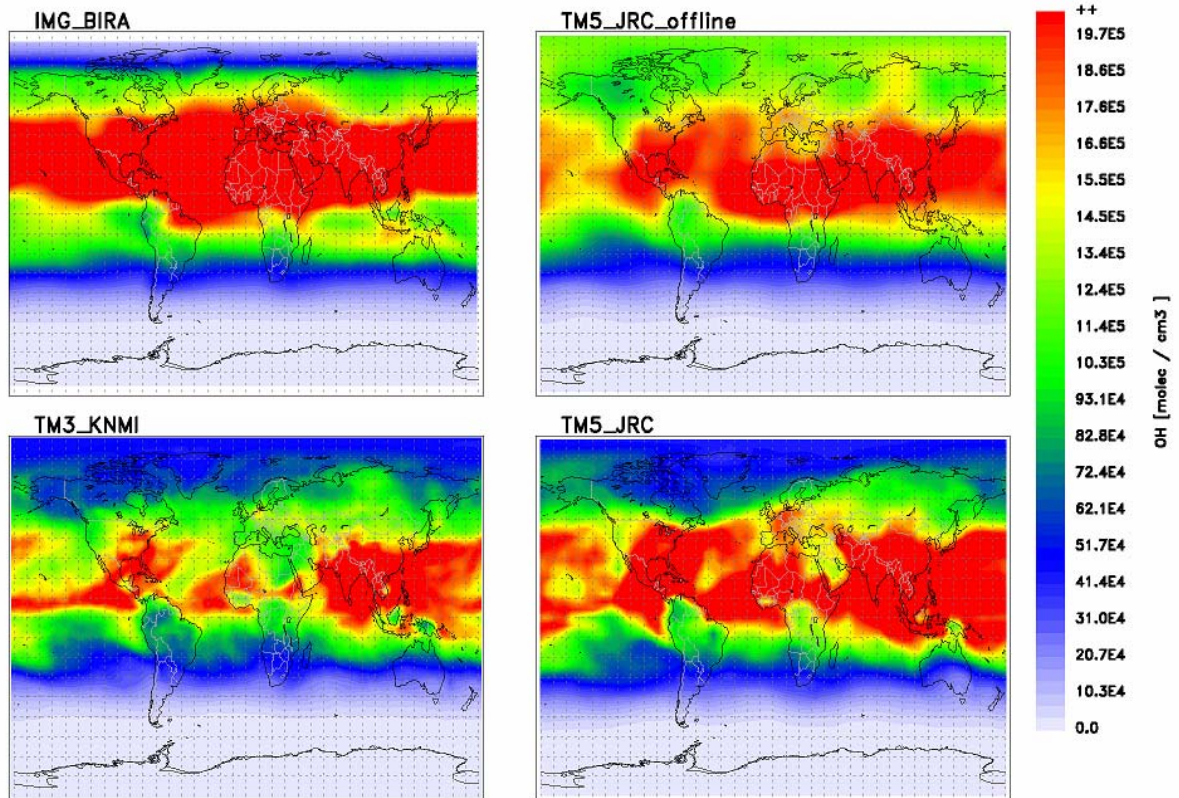
500.000hPa   December
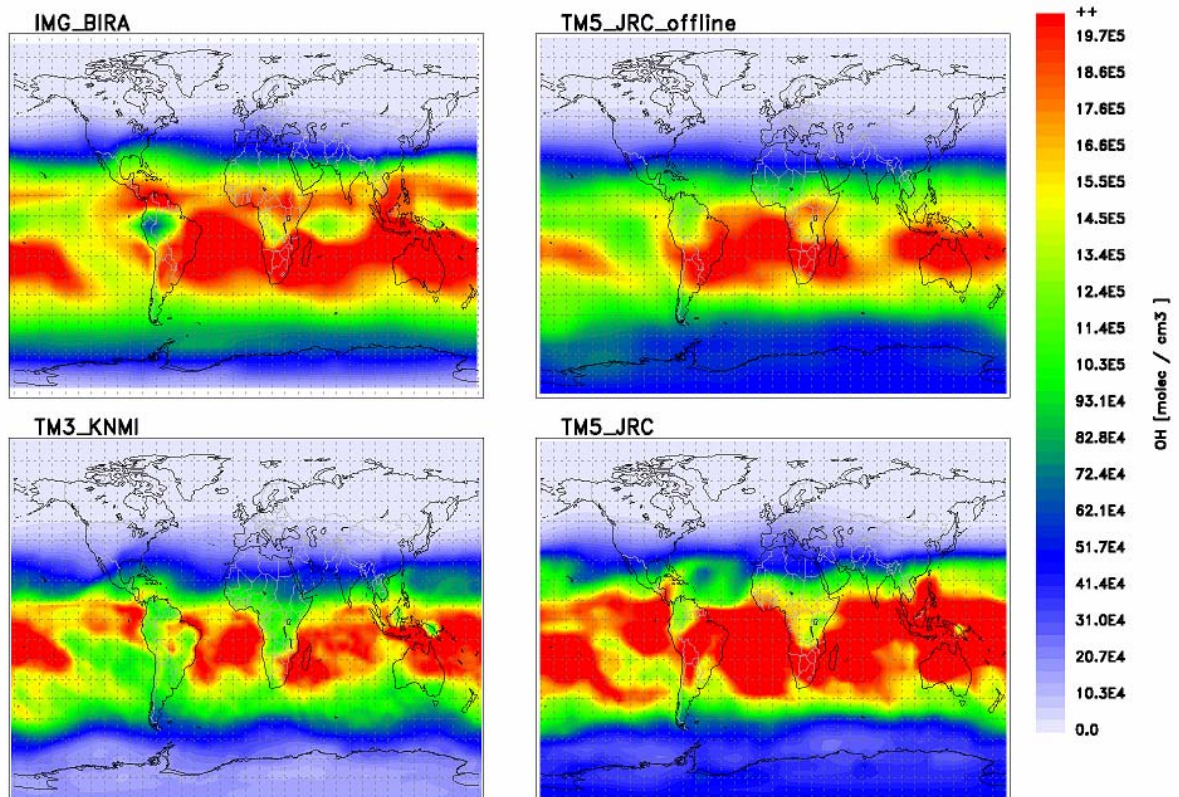
Figure 6.2: OH intercomparison: free troposphere (500 hPa) (top: June; bottom: December).
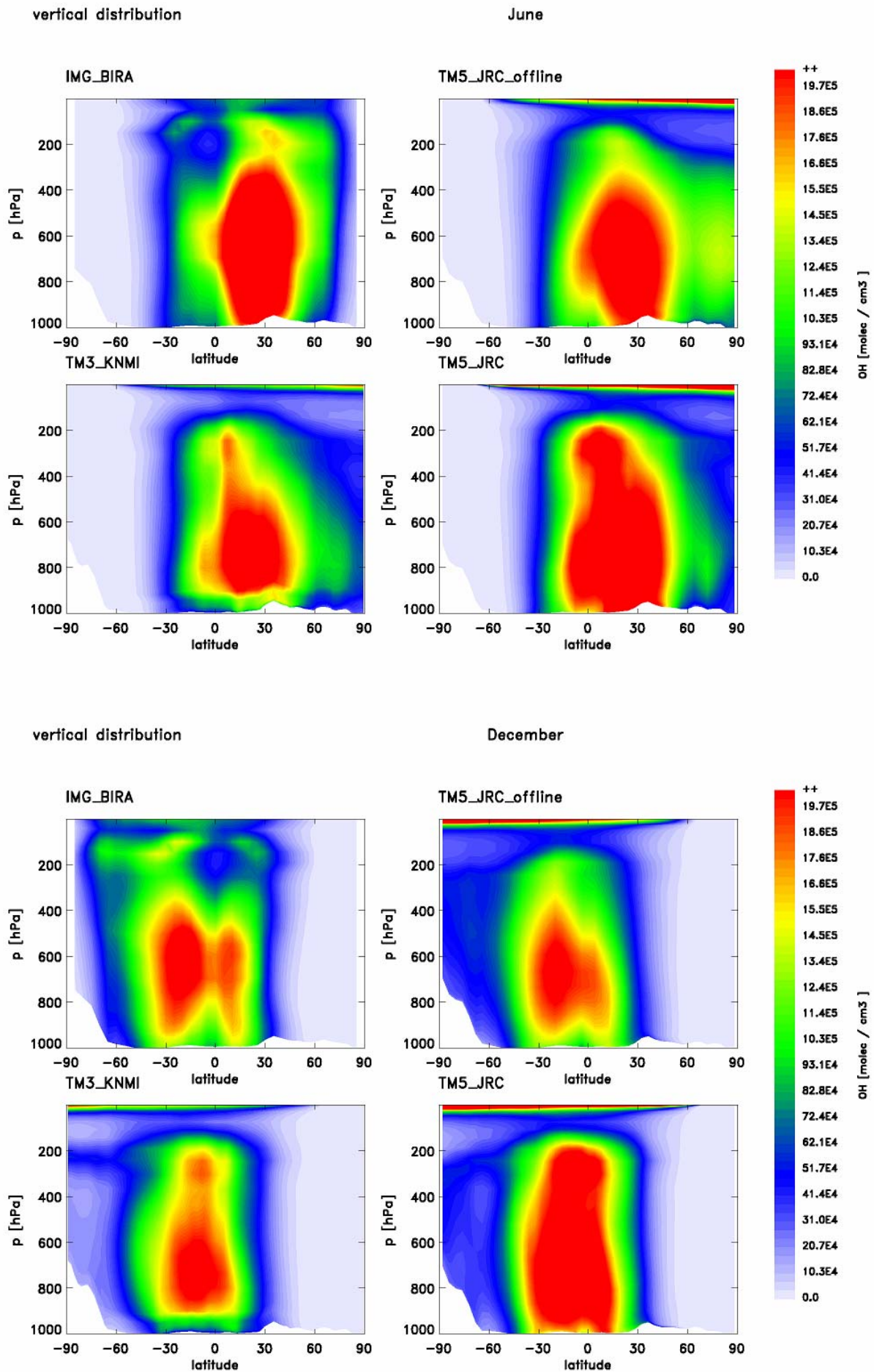
Figure 6.3: OH intercomparison: vertical distribution (latitudinal averages) (top: June; bottom: December).

7   References

Bergamaschi, P., C. Frankenberg, J.F. Meirink, M. Krol, F. Dentener, T. Wagner, U. Platt, J.O. Kaplan, S. Körner, M. Heimann, E.J. Dlugokencky, and A. Goede, Satellite chartography of atmospheric methane from SCIAMACHY onboard ENVISAT: (II) Evaluation based on inverse model simulations, *J. Geophys. Res., submitted*, 2006.

Bergamaschi, P., M. Krol, F. Dentener, A. Vermeulen, F. Meinhardt, R. Graul, M. Ramonet, W. Peters, and E.J. Dlugokencky, Inverse modelling of national and European CH_4 emissions using the atmospheric zoom model TM5, *Atmos. Chem. Phys.*, *5*, 2431-2460, 2005.

Brühl, C., and P.J. Crutzen, The MPIC 2D model, in *NASA Ref. Publ. 1292, vol1*, pp. 103-104, 1993.

Costen, R.C., G.M. Tennille, and J.S. Levine, Cloud pumping in a one-dimensional model, *J. Geophys. Res.*, *93*, 15,941-15,954, 1988.

Denning, A.S., M. Holzer, K.R. Gurney, M. Heimann, R.M. Law, P.J. Rayner, I.Y. Fung, S.-M. Fan, S. Taguchi, P. Friedlingstein, Y. Balkanski, M. Maiss, and I. Levin, Three-dimensional transport and concentration of SF6: A model intercomparison study (TransCom 2), *Tellus*, *51B*, 266-297, 1999.

Dentener, F., M. van Weele, M. Krol, S. Houweling, and P. van Velthoven, Trends and inter-annual variability of methane emissions derived from 1979-1993 global CTM simulations, *Atmos. Chem. Phys.*, *3*, 73-88, 2003.

Hauglustaine, D.A., F. Hourdin, L. Jourdain, M.A. Filiberti, S. Walters, J.F. Lamarque, and E.A. Holland, Interactive chemistry in the Laboratoire de Meteorologie Dynamique general circulation model: Description and background tropospheric chemistry evaluation, *J. Geophys. Res., 109*, doi:10.1029/2003JD003957, 2004.

Heimann, M., and S. Koerner, The Global Atmospheric Tracer Model TM3. Model Description and Users Manual Release 3.8a, No.5, Max Planck Institute for Biogeochemistry (MPI-BGC), Jena, Germany, 2003.

Holtslag, A.A.M., and C.-H. Moeng, Eddy diffusivity and counter-gradient transport in the convective atmospheric boundary layer, *J. Atmos. Sci.*, *48*, 1690-1698, 1991.

Hourdin, F., F. Couvreux, and L. Menut, Parameterization of the dry convective boundary layer based on a mass flux representation of thermals, *Journal of the Atmospheric Sciences*, *59*, 1105-1123, 2002.

IPCC, Climate Change 2001: The scientific basis, Cambridge University Press, 2001.

Krol, M.C., S. Houweling, B. Bregman, M. van den Broek, A. Segers, P. van Velthoven, W. Peters, F. Dentener, and P. Bergamaschi, The two-way nested global chemistry-transport zoom model TM5: algorithm and applications, *Atmos. Chem. Phys.*, *5*, 417-432, 2005.

Louis, J.F., A parametric model of vertical eddy fluxes in the atmosphere, *Boundary Layer Meteorology*, *17*, 187-202, 1979.

Muller, J.F., and G.P. Brasseur, IMAGES: A three-dimensional chemical transport model of the global troposphere, *J. Geophys. Res.*, *100*, 16,445-16,490, 1995.

Patra, P.K., S. Lal, B.H. Subbaraya, C.H. Jackman, and P. Rajaratnam, Observed vertical profile of sulphur hexafluoride (SF_6) and its atmospheric applications, *J. Geophys. Res.*, *102*, 8855-8859, 1997.

Rinsland, C.P., C. Boone, R. Nassar, K. Walker, P. Bernath, J.C. McConnell, and L. Chiou, Trends of HF, HCl, CCl_2F_2, CCl_3F, $CHClF_2$ (HCFC-22), and SF_6 in the

lower stratosphere from Atmospheric Chemistry Experiment (ACE) and Atmospheric Trace Molecule Spectroscopy (ATMOS) measurements near 30°N latitude, *Geophys. Res. Lett.*, *32*, doi:10.1029/2005GL022415, 2005.

Russell, G.L., and J.A. Lerner, A new finite-differencing scheme for the tracer transport equation, *Journal of Applied Meteorology*, *20*, 1483-1498, 1981.

Smolarkiewicz, P.K., and P.J. Rasch, Monotone advection on the sphere: An Eulerian versus semi-Lagrangian approach, *J. Atmos. Sci.*, *48*, 793-810, 1991.

Tiedtke, M., A comprehensive mass flux scheme for cumulus parameterization in large-scale models, *Monthly Weather Review*, *117*, 1779-1800, 1987.

Abstract

A comprehensive inter-comparison of 5 atmospheric chemistry transport models (TM5, TM4, TM3, IMAGES, and LMDZ) has been performed. The main objective was to analyze differences in model transport, in particular vertical mixing (boundary layer and convective transport), synoptic variations, and large scale global circulation (including inter-hemispheric exchange and stratospheric tropospheric exchange (STE)). For this purpose simulations of various tracers with very different atmospheric lifetimes τ have been carried out: ^{222}Rn ($\tau = 3.8$ days), SF_6 ($\tau = \sim3000$ years), and CH_4 ($\tau = \sim9$ years), using prescribed boundary conditions for all models. Furthermore, OH fields from various model simulations with full chemistry have been compared.

EUROPEAN COMMISSION
DIRECTORATE-GENERAL
Joint Research Centre

The mission of the JRC is to provide customer-driven scientific and technical support for the conception, development, implementation and monitoring of EU policies. As a service of the European Commission, the JRC functions as a reference centre of science and technology for the Union. Close to the policy-making process, it serves the common interest of the Member States, while being independent of special interest, whether private or national.

Publications Office
Publications.eu.int